Supplementary Information (SI) for Journal of Materials Chemistry A.
This journal is © The Royal Society of Chemistry 2025

Supplementary information (SI)

A High-Performance Low-Sensitivity Explosive LX-11: Benefited by a *N*-NH_2 Side-Arm Hydrogen Bonding

Shaoqing Wang,[a] Shaojia Li,[a] Jialin Wang,[a] Ziang, Wang,[a] Hongquan Yin,[a] Qing Ma[b] and Fu-Xue Chen*[a]

a. School of Chemistry & Chemical Engineering, Beijing Institute of Technology (Liangxiang Campus), Beijing 102488, China.

b. Institute of Chemical Materials, CAEP, Mianyang 621050, China.

E-mail addresses: fuxue.chen@bit.edu.cn (Fu-Xue Chen).

Contents

1. Experimental Sections

Safety Caution! All the nitrogen-rich compounds may explode under certain conditions although no explosion was encountered in the procedure of preparing these energetic materials. Thus, it is indispensable to keep safeguard procedures and keep experiments in a small scale at the same time.

Characterization methods ^{1}H NMR, ^{13}C NMR and ^{15}N NMR spectra were recorded on Buruker Avance nuclear magnetic resonance spectrometers operating at 400 MHz, 100 MHz, and 700 MHz, respectively. Chemical shifts are reported in ppm relative to Me_4Si. Differential scanning calorimeter (DSC, Shimadzu TA-60ws) was used to measure the melting temperatures and decomposition temperatures at a heating rate of 10 °C min^{-1} under argon atmosphere. IR spectra were recorded using KBr pellets for solids on a Bruker ALPHA FT-IR Spektrometer. HRMS was recorded on Bruker Apex IV FTMS. Elemental analyse was recorded on FlashSmarte. All chemicals were bought from commercial companies and used directly unless otherwise noted. The sensitivities towards impact and friction were determined using a drop hammer and a BAM friction tester. Densities were determined at room temperature by employing a Micromeritics AccuPyc 1340 gas pycnometer. X-Ray diffractions of all single crystals were carried out on a Bruker D8 VENTURE diffractometer using Mo-Kα radiation (λ = 0.71073 Å).

Compound 3: Compound **2** (178 mg, 0.7 mmol, 1 eq.) was dissolved in water (7.0 mL), followed by the addition of sodium hydroxide (NaOH, 763 mg, 6.7 mmol, 9.6 eq.), aqueous solution of Hydroxylamine-*O*-sulfonic acid (NH_2OSO_3H) (191 mg, 4.8 mmol, 6.8 eq., 3.0 mL). Allowing the reaction to proceed overnight at room temperature, the mixture was filtered to yield a light yellow solid, 151 mg (84%). $T_{d\,(onset)}$=260.6 °C. ^{1}H NMR (400 MHz, DMSO-d_6): δ 14.18 (s, 2H, NH), 9.90 (s, 2H, NH) ppm. ^{13}C NMR (100 MHz, DMSO-d_6): δ 161.4, 158.7, ppm. ^{15}N NMR (700 MHz, DMSO-d_6): δ 357.2, 276.9, 203.6, 185.1, 87.5 ppm. IR: 3591 (s), 3422 (s), 3198 (m), 1624 (m), 1528 (m), 1412 (s), 1304 (s) cm^{-1}. HRMS: calcd. for $C_4H_5N_{10}O_4$ $[M + H]^+$: 257.0490, found: 257.0489. Elemental Analysis calcd. for $C_4H_4N_{10}O_4$: C 18.76, H 1.57, N 54.68, found: C 18.54, H 1.63, N 54.35.

Compound LX-11: Compound **3** (178 mg, 0.7 mmol, 1 eq.) was dissolved in acetonitrile (8.0 mL), followed by the addition of NaOH (88 mg, 2.2 mmol, 2.2 eq.), and the reaction was carried out at 50 °C for 10 min. After cooling to room temperature, azanyl 2,4,6-trimethylbenzenesulfonate (MSH, 409 mg, 1.9 mmol, 1.9 eq.) was added, and the reaction continued at room temperature for 20 min. Subsequently, *N*-bromosuccinimide (NBS, 214 mg, 1.2 mmol, 1.2 eq.) was added, and the reaction proceeded for an additional 1 h. The mixture was filtered, and the filtrate was subjected to extraction with ethyl acetate (3×50 mL). The collected organic layers were washed with saturated sodium chloride (3×50 mL) and concentrated under vacuum. The crude product was purified by column chromatography on silica gel, eluting with ethyl acetate/petroleum ether (v/v, 5:1) to afford **LX-11** as a light-yellow solid, 85 mg (30%). $T_{d\,(onset)}$ = 201.36 °C. ^{1}H NMR (400 MHz, DMSO-d_6): δ 7.80 (s, 2H, NH) ppm. ^{13}C NMR (100 MHz, DMSO-d_6): δ 16.1, 158.3, 156.2, 141.0 ppm. ^{15}N NMR (700 MHz, DMSO-d_6): δ 353.0, 351.1, 330.4, 303.4, 285.7, 280.0, 259.5, 251.4, 236.7, 222.5, 199.0, 88.5 ppm. IR: 3347 (s), 3281 (m), 1566 (m), 1418 (m), 1331 (m), 1315 (s), 11192 (s), 1098 (s) cm^{-1}. HRMS: calcd. for $C_4H_3N_{12}O_4$ $[M - H]^-$: 283.0406, found: 283.0395. Elemental Analysis calcd. for $C_4H_4N_{12}O_4$: C 16.91, H 1.42, N 59.19, found: C 18.47, H 2.29, N 59.03.

Compound 6: Compound **4** (72 mg, 0.5 mmol, 1.0 eq.) was dissolved in CH_3CN (3.0 mL), followed by the addition of isoamyl nitrite (135 mg, 1.15 mmol, 2.3 eq.), then react for 3 hours. After

completing the reaction, the solvent was evaporated to dryness. Ethyl acetate and petroleum ether were added for recrystallization. The mixture was filtered, yielding a light yellow solid, 36 mg (63%). ^{1}H NMR (400 MHz, DMSO-d_6): δ 15.27 (s, 2H, NH), 8.89 (s, 2H, NH) ppm. ^{13}C NMR (100 MHz, DMSO-d_6): δ 163.6, 146.8, ppm. HRMS: calcd. for C_2HN_4O [M – H]$^-$: 113.0105, found: 113.0108. ***Safety Caution! During workup, a slight explosion occurred.***

2. Optimization experiments

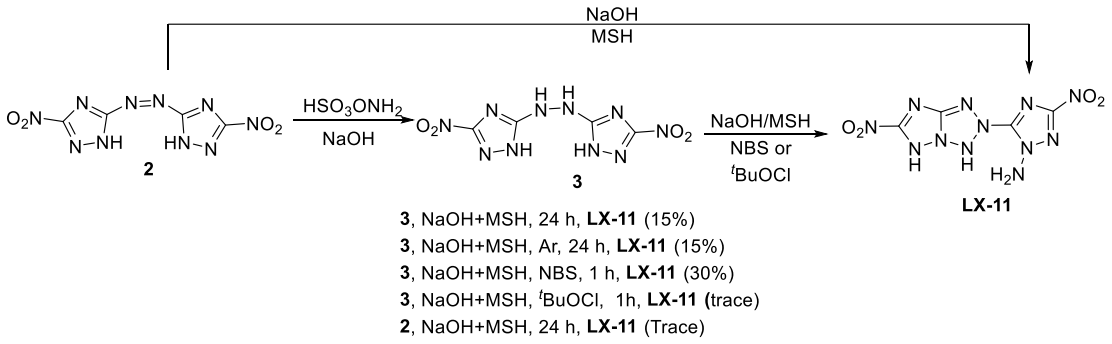

Scheme S1 Optimization experiments for the preparation of **LX-11**.

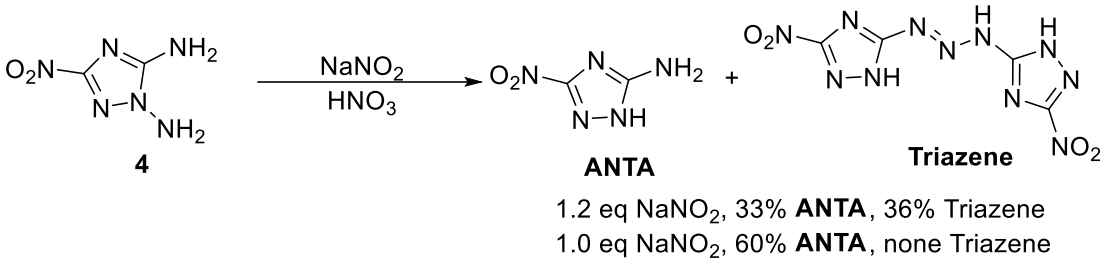

Scheme S2 The reaction of **4** with sodium nitrite.

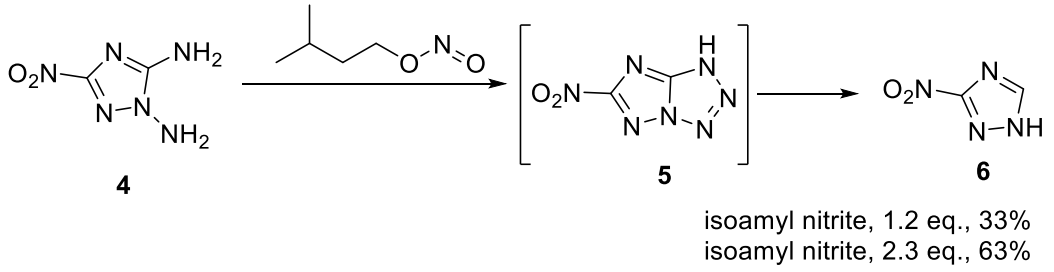

Scheme S3 The reaction of **4** with isoamyl nitrite.

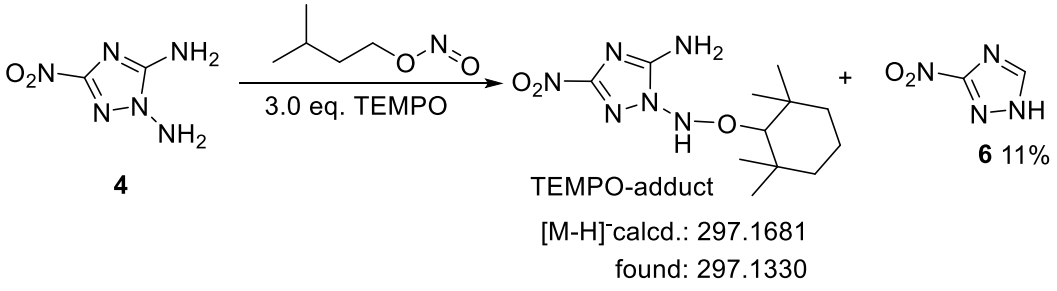

Scheme S4 The control experiment with TEMPO.

3. Gaussian Calculations

Theoretical calculations were performed by using the Gaussian 09 (Revision D.01) suite of programs. [1] The elementary geometric optimization and the frequency analysis were performed at the level of the Becke three parameter, Lee-Yan-Parr (B3LYP) functional with the 6-311G** basis set. All of the optimized structures were characterized to be local energy minima on the potential surface without any imaginary frequencies. Atomization energies were calculated by the CBS-4M. All the optimized structures were characterized to be true local energy minima on the potential-energy surface without imaginary frequencies. [2]

The predictions of heat of formation (HOF) adopt the hybrid DFT-B3LYP methods with 6-311G** basis set via designed isodesmic reactions. The isodesmic reactions used to derive the HOF of as-synthesized compounds are in Scheme S5.

The change of enthalpy for the reactions at 298 K can be expressed as following:

$$\Delta H_{298} = \sum \Delta_f H_P - \sum \Delta_f H_R \quad (1)$$

Where $\sum \Delta_f H_P$ and $\sum \Delta_f H_R$ are the HOF of reactants and products at 298 K, respectively, and ΔH_{298} can be calculated using the following expression:

$$\Delta H_{298} = \Delta E_{298} + \Delta(PV) = \Delta E_0 + \Delta ZPE + \Delta H_T + \Delta nRT \quad (2)$$

Where ΔE_0 is the change in total energy between the products and the reactants at 0 K; ΔZPE is the difference between the zero-point energies (ZPE) of the products and the reactants at 0 K; ΔH_T is thermal correction from 0 to 298 K. The $\Delta(PV)$ value in Equation 2 is the PV work term. It equals $\Delta(nRT)$ for the reactions of ideal gas. For the isodesmic reaction, $\Delta n = 0$, so $\Delta(PV) = 0$. On the left side of Equation 1, apart from target compound, all the others are called reference compounds. The HOF of reference compounds is available either from the experiments or from the high-level computing such as CBS-4M.

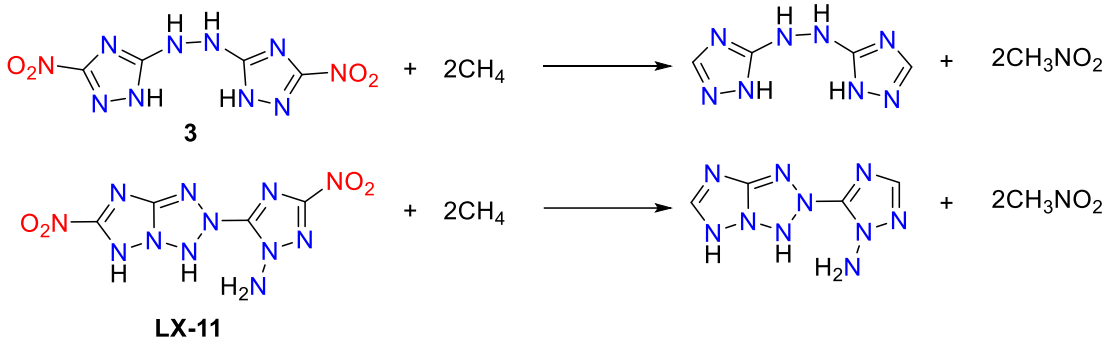

Scheme S5 Isodesmic reactions for neutral compounds

For the solid phase species, enthalpies of formation ΔH_f (s) can be estimated following the Trouton's rule[3]:

$$\Delta H_{sub} = 188/\text{J mol-1K-1T} \quad (3)$$

$$\Delta H_f(s) = \Delta H_f(g) - \Delta H_{sub} \quad (4)$$

ΔH_{sub} = sublimation enthalpy; ΔH_f (g) = the heats of formation for gas-phase; ΔH_f (s) = the heats of formation for solid-phase. Here, T represents the melting point or the decomposition temperature when no melting point occurs prior to decomposition.

Table S1 Calculated zero-point energy (ZPE), thermal correction to enthalpy (HT), total energy (E0) and heats of formation (HOF)

Compound	E_0 / a. u	ZPE / kJ mol^{-1}	ΔH_T / kJ mol^{-1}	HOF/kJ mol^{-1}

E3	-1003.08108	363.37	40.94	498.1
E4	-1112.444942	386.73	45.06	960.0
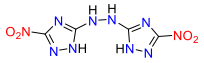	-593.980412	342.89	25.47	544.0
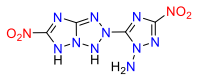	-703.365862	377.60	30.41	961.1
CH_4	-40.489173	117.02	10.01	-74.6
CH_3NO_2	-245.032025	130.38	11.60	-81.0

The sublimation enthalpy, the gas- and solid-phase heats of formation of compounds **E3** and **E4** were calculated below:

Table S2 The Heats of Formation for Gas-, Solid-Phase and Heats of Phase Change for compound **E3** and **E4**.

Compound	ΔH_{sub}/kJ·mol^{-1}	ΔH_f (g)/kJ·mol^{-1}	ΔH_f (s)/kJ·mol^{-1}
E3	100.4	498.1	397.7
E4	90.0	960.0	870.0

4. Thermal decomposition kinetics of LX-11

To investigate the thermal decomposition kinetics of **LX-11** and obtain its thermal decomposition kinetic parameters and activation energy, a DSC curve analysis was performed on **LX-11** at heating rates of 2.5, 5, 10·min^{-1} over a temperature range of 60-300 °C. See Figure S1 for the detailed DSC curves.

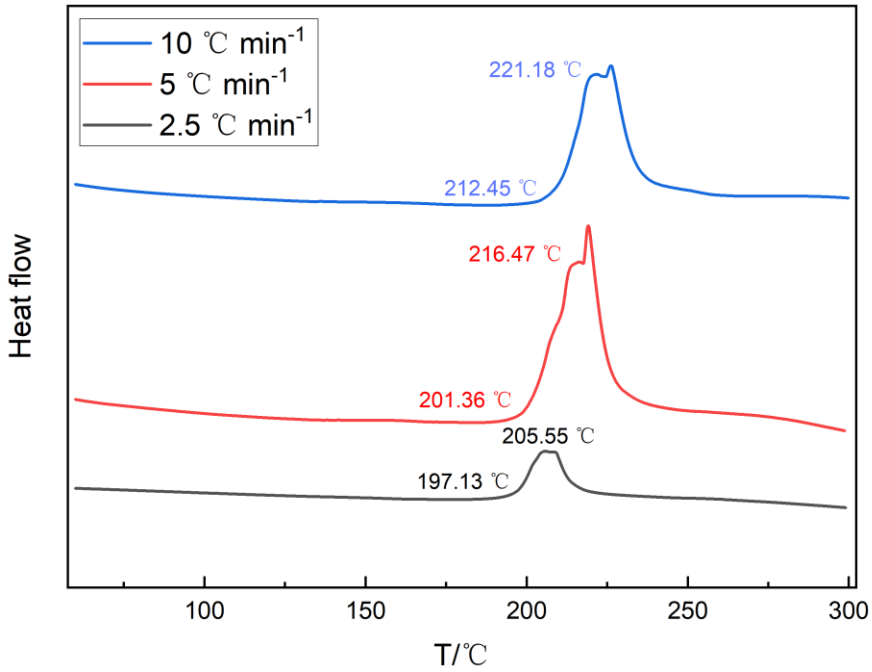

Figure S1 DSC curves of LX-11 at different heating rates.

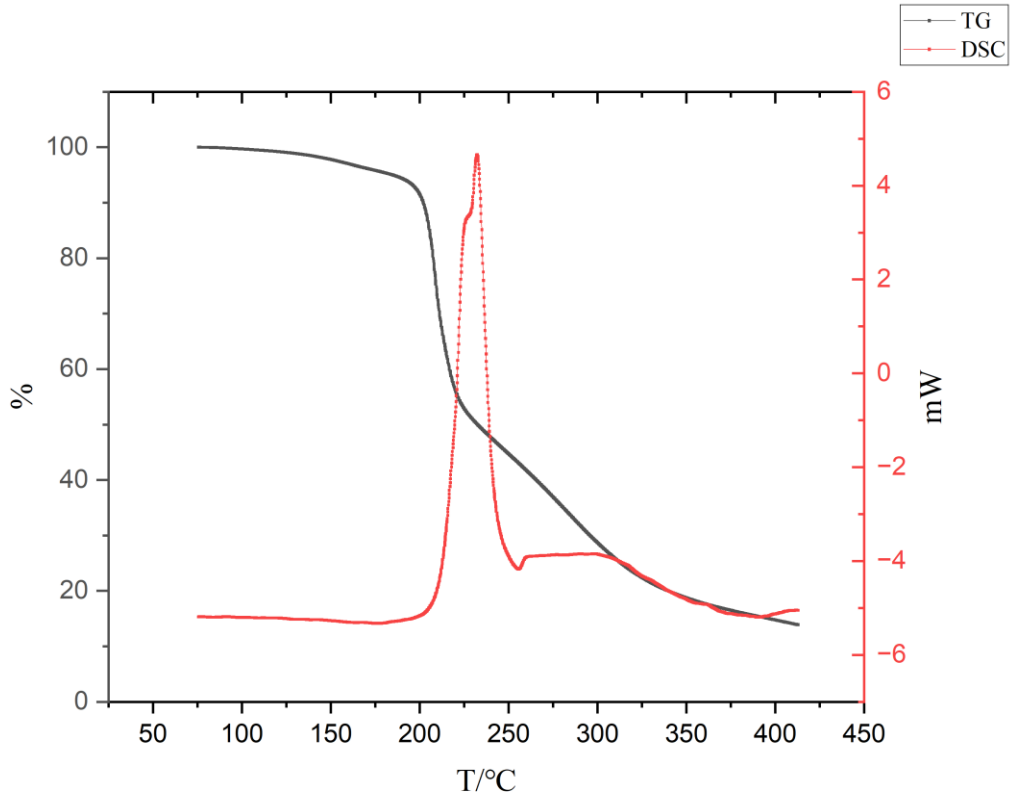

Figure S2 DSC-TG curves of LX-11.

As shown in Figure 1, the DSC curve of compound LX-11 shifts significantly to the right with an increase in the heating rate, resulting in an elevation of the decomposition temperature. It was observed that at heating rates of 2.5, 5, 10, °C·min^{-1}, **LX-11** exhibited two distinct decomposition peaks, indicative of secondary decomposition. At a heating rate of 15 °C·min^{-1}, due to the rapid increase in heating rate, the first decomposition peak was not observed, and the compound immediately underwent the second decomposition, showing only a change in the slope of the curve. The apparent activation energies were calculated based on the peak temperatures (T_p) corresponding to different heating rates using multiple scanning rate methods (the Kissinger method (Equation 5) and the Ozawa method (Equation 6)).

The Kissinger method equation is as follows:

$$\ln\left[\beta / T_P^{\,2}\right] = \ln\left[AR / E_a\right] - \ln\left[E_a / RT_P\right] \tag{5}$$

where β is the heating rate, K·min^{-1}; T_p is the decomposition peak temperature, K; E_a is the apparent activation energy, kJ·mol^{-1}; A is the pre-exponential factor, S^{-1}; R is the gas constant, 8.314 J·K^{-1}·min^{-1}.

The Ozawa method equation is as follows:

$$\ln \beta = C - 0.4567 E_a / RT \tag{6}$$

where C=lg[AE_a/RG(α)]-2.315, and G(α) is the integral function of the reaction mechanism.

Linear regression analysis was performed for ln(β/T_p^2)-1/T_p×10^3 and lgβ-1/T_p×10^3,

and the apparent activation energy E_a of **LX-11** was calculated from the slopes of the straight lines. The pre-exponential factor lnA was determined from the intercepts using the Kissinger method. Specific data are presented in Table S1. It was found that the results obtained from the Kissinger method and the Ozawa method are consistent.

Table S3 Kinetic parameters obtained by Kissinger and Ozawa method

β/K·min^{-1}	T_P/K	Kissinger method			Ozawa method	
		E_K/kJ·mol^{-1}	lnA	r	E_o/kJ·mol^{-1}	r
2.5	205.55					
5	216.47	157.124	30.940	0.9415	157.101	0.9468
10	221.18					

5. Crystallographic data

5.1 Single crystal structure of 3

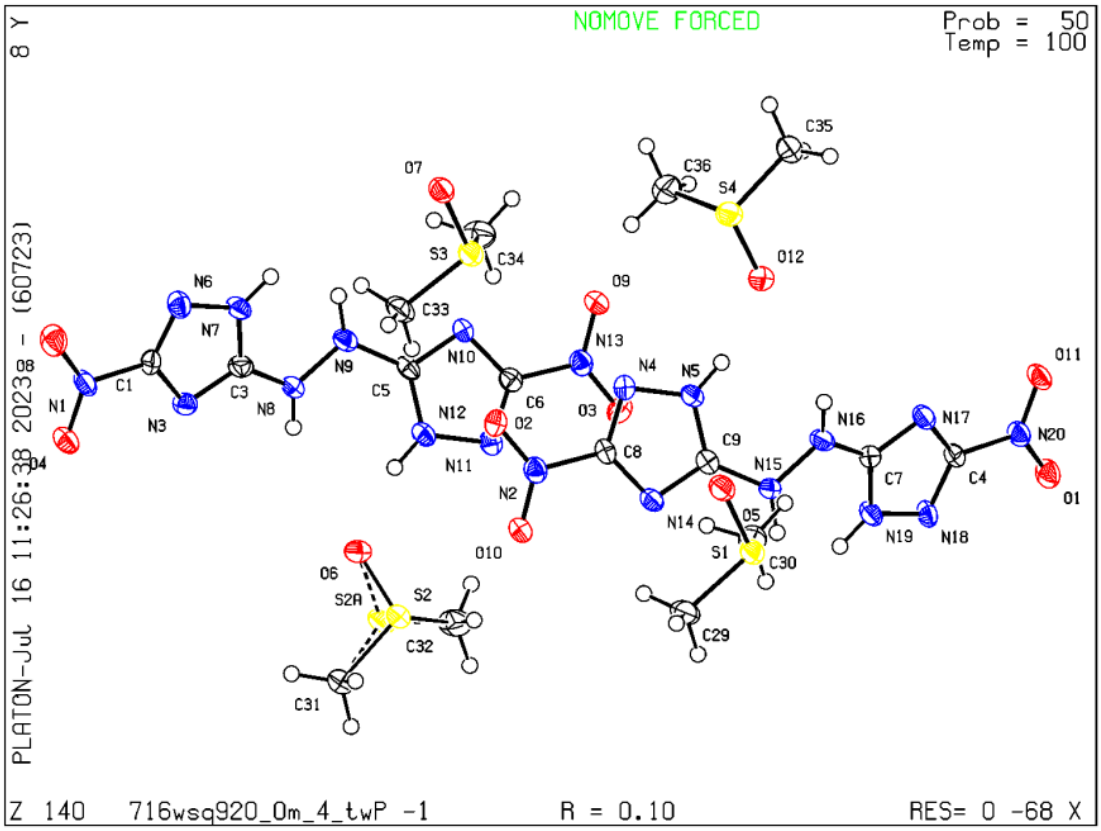

Figure S3 Crystal structures of compound **3**·2DMSO.

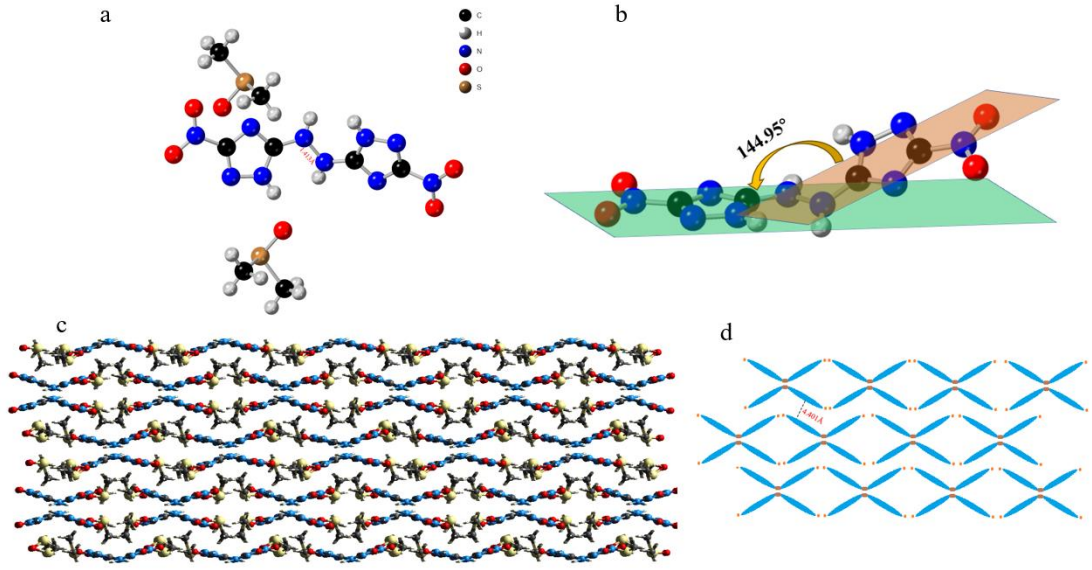

Figure *S4* (a) The crystal structure of **3**·2DMSO; (b) The planarity of **3**; (c) The crystal packing diagrams of **3**·2DMSO; (d) Schematic diagram of the crystal packing of **3**·2DMSO.

Table S4 Crystal data and structure refinement for compound **3**·2DMSO.

Compound	**3**·2DMSO
Formula	$C_4H_4N_{10}O_4 \cdot C_4H_{12}O_2S_2$
M_w[g mol^{-1}]	412.03
T[K]	100
Wavelength	0.71073 Å
Crystal system	triclinic
Space group	*P*-1
a[Å]	11.1210(9)
b[Å]	12.404(1)
c[Å]	12.4946(9)
α[°]	86.939(2)
β[°]	86.578(3)
γ[°]	88.148(3)
V[Å^3]	1717.3(2)
Z	4
$\rho_{calc.}$[g cm^{-3}]	1.595
Absorption coefficient [mm^{-1}]	0.363
F[000]	856.0
Crystal size[mm^3]	0.130 x 0.120 x 0.090
Theta range for data collection [°]	4.518 to 52.952
Index ranges	-13≤h≤13, -15≤k≤15, -13≤I≤15
Reflections collected	7040
Data/restraints/parameters	7040/12/486
Final *R* index[$I > 2\sigma(I)$]	R_1 = 0.1035, wR_2 = 0.2501
R indices (all data)	R_1 = 0.1477, wR_2 = 0.2779
Goodness-of-fit on F^2	1.159
CCDC	2386021

Table S5 Crystal Atomic coordinates (x 10^4) and equivalent isotropic displacement parameters (Å^{2}x 10^3) for compound **3** U(eq) is defined as one third of the trace of the orthogonalized U^{ij} tensor.

	x	y	z	U(eq)
S1	4584.9(12)	8933.1(10)	1153.5(10)	24.6(3)

S3	4511.2(12)	3857.3(11)	6186.8(10)	26.3(4)
S4	516.1(12)	3966.1(11)	3899.4(10)	27.4(4)
O1	-981(3)	3408(3)	-3322(3)	30.3(9)
O2	6058(3)	3552(3)	3519(3)	27.2(8)
O3	3985(3)	1553(3)	1504(3)	29.6(9)
O4	11881(3)	954(3)	6977(3)	27.1(8)
O5	4277(3)	8950(3)	2352(3)	28.5(8)
O6	9187(3)	1503(3)	2486(3)	34.5(10)
O7	4198(3)	3906(3)	7379(3)	27.7(8)
O8	10942(3)	1169(3)	8538(3)	34.6(10)
O9	3042(3)	1200(3)	3052(3)	25.8(8)
O10	6969(3)	3872(3)	1942(3)	27.2(8)
O11	-1928(3)	3749(3)	-1797(3)	26.9(8)
O12	810(3)	3996(3)	2695(3)	31.4(9)
N1	10976(4)	1031(4)	7566(3)	26.7(10)
N2	6070(4)	3778(3)	2542(3)	24(1)
N3	9802(4)	698(3)	6044(3)	22.4(9)
N4	3902(4)	3737(3)	2644(3)	24(1)
N5	3089(4)	3952(3)	1872(3)	21.4(9)
N6	8805(4)	1133(4)	7613(3)	25.8(10)
N7	8007(4)	981(3)	6850(3)	23.7(10)
N8	8106(4)	521(3)	5002(3)	24.1(10)
N9	6851(4)	514(3)	5048(3)	23.6(10)
N10	5153(4)	822(3)	4002(3)	20.9(9)
N11	6112(4)	1431(3)	2440(3)	24.6(10)
N12	6919(4)	1205(3)	3204(3)	23(1)
N13	3955(4)	1321(3)	2466(3)	23.2(9)
N14	4856(4)	4215(3)	1033(3)	22.3(9)
N15	3133(4)	4508(3)	2(3)	21.5(9)
N16	1861(4)	4494(3)	63(3)	23.2(10)
N17	160(4)	4115(3)	-909(3)	23.9(10)
N18	1155(4)	3580(3)	-2455(3)	23.7(10)
N19	1956(4)	3843(3)	-1724(3)	23.8(10)
N20	-1009(4)	3627(3)	-2381(3)	24(1)
C1	9827(5)	945(4)	7081(4)	22.5(11)
C3	8610(5)	722(4)	5940(4)	23.9(11)
C4	134(5)	3770(4)	-1901(4)	22.1(11)
C5	6337(4)	834(4)	4111(4)	20.1(11)
C6	5099(5)	1193(4)	2964(4)	20.6(11)
C7	1353(5)	4164(4)	-823(4)	21.4(11)
C8	4909(4)	3906(4)	2068(4)	21.0(11)
C9	3660(5)	4241(4)	937(4)	21.6(11)
C29	6189(5)	8858(5)	1056(4)	33.3(13)
C30	4289(5)	7604(4)	783(4)	30.7(13)
C31	10932(5)	1744(5)	1033(4)	33.1(13)
C32	8662(5)	1516(6)	462(4)	41.5(16)
C33	6086(5)	3604(5)	6116(4)	36.4(14)
C34	4054(5)	2566(5)	5822(4)	37.3(14)
C35	-1067(5)	3827(5)	4045(4)	36.9(14)
C36	948(5)	2646(5)	4382(4)	37.5(14)
S2A	9620(18)	1134(16)	1142(17)	28(4)
S2	9441.8(12)	2175.2(11)	1443.2(11)	25.6(4)

Table S6 Bond lengths [Å] for compound **3**.

Atom	Atom	Length/Å	Atom	Atom	Length/Å
S1	O5	1.517(3)	N6	C1	1.303(6)
S1	C29	1.780(5)	N7	C3	1.335(6)
S1	C30	1.782(5)	N8	N9	1.394(6)

S3	O7	1.514(3)	N8	C3	1.367(6)
S3	C33	1.767(5)	N9	C5	1.368(6)
S3	C34	1.786(6)	N10	C5	1.333(6)
S4	O12	1.519(3)	N10	C6	1.356(6)
S4	C35	1.772(6)	N11	N12	1.361(5)
S4	C36	1.775(5)	N11	C6	1.303(6)
O1	N20	1.219(5)	N12	C5	1.338(6)
O2	N2	1.237(5)	N13	C6	1.450(6)
O3	N13	1.219(5)	N14	C8	1.333(6)
O4	N1	1.215(5)	N14	C9	1.341(6)
O6	S2A	1.80(2)	N15	N16	1.413(6)
O6	S2	1.525(4)	N15	C9	1.360(6)
O8	N1	1.233(5)	N16	C7	1.360(6)
O9	N13	1.225(5)	N17	C4	1.335(6)
O10	N2	1.219(5)	N17	C7	1.341(6)
O11	N20	1.229(5)	N18	N19	1.372(5)
N1	C1	1.456(6)	N18	C4	1.315(6)
N2	C8	1.452(6)	N19	C7	1.348(6)
N3	C1	1.348(6)	N20	C4	1.458(6)
N3	C3	1.339(7)	C31	S2A	1.66(2)
N4	N5	1.371(5)	C31	S2	1.780(5)
N4	C8	1.311(6)	C32	S2A	1.45(2)
N5	C9	1.334(6)	C32	S2	1.790(6)
N6	N7	1.364(5)			

Table S7 Bond angles [°] for compound **3**.

Atom	**Atom**	**Atom**	**Angle/°**	**Atom**	**Atom**	**Atom**	**Angle/°**
O5	S1	C29	103.7(2)	O1	N20	O11	125.4(4)
O5	S1	C30	106.1(2)	O1	N20	C4	117.9(4)
C29	S1	C30	99.2(3)	O11	N20	C4	116.7(4)
O7	S3	C33	103.5(2)	N3	C1	N1	120.1(5)
O7	S3	C34	106.0(2)	N6	C1	N1	121.7(4)
C33	S3	C34	98.4(3)	N6	C1	N3	118.2(5)
O12	S4	C35	104.7(2)	N3	C3	N8	123.0(4)
O12	S4	C36	105.6(2)	N7	C3	N3	111.3(5)
C35	S4	C36	98.1(3)	N7	C3	N8	125.7(5)
O4	N1	O8	126.0(5)	N17	C4	N20	120.7(5)
O4	N1	C1	117.0(4)	N18	C4	N17	119.3(5)
O8	N1	C1	117.1(4)	N18	C4	N20	120.0(4)
O2	N2	C8	116.9(4)	N10	C5	N9	122.7(4)
O10	N2	O2	125.6(4)	N10	C5	N12	111.2(4)
O10	N2	C8	117.5(4)	N12	C5	N9	126.2(4)
C3	N3	C1	100.0(4)	N10	C6	N13	121.0(4)
C8	N4	N5	99.8(4)	N11	C6	N10	117.4(5)
C9	N5	N4	110.2(4)	N11	C6	N13	121.7(4)
C1	N6	N7	101.1(4)	N17	C7	N16	123.6(4)
C3	N7	N6	109.4(4)	N17	C7	N19	110.7(4)
C3	N8	N9	115.6(4)	N19	C7	N16	125.7(5)
C5	N9	N8	115.0(4)	N4	C8	N2	121.2(4)
C5	N10	C6	100.5(4)	N4	C8	N14	118.9(5)
C6	N11	N12	101.6(4)	N14	C8	N2	119.8(5)
C5	N12	N11	109.4(4)	N5	C9	N14	110.5(4)
O3	N13	O9	125.7(4)	N5	C9	N15	125.9(4)
O3	N13	C6	117.3(4)	N14	C9	N15	123.6(4)
O9	N13	C6	117.0(4)	C31	S2A	O6	97.0(11)
C8	N14	C9	100.5(4)	C32	S2A	O6	107.3(12)
C9	N15	N16	115.2(4)	C32	S2A	C31	119.4(12)
C7	N16	N15	115.6(4)	O6	S2	C31	103.0(2)

C4	N17	C7	100.3(4)	O6	S2	C32	104.6(3)
C4	N18	N19	99.9(4)	C31	S2	C32	97.9(3)
C7	N19	N18	109.8(4)				

Table S8 Torsion Angles [°] for compound **3**.

A	B	C	D	Angle/°	A	B	C	D	Angle/°
O1	N20	C4	N17	173.2(4)	N12	N11	C6	N13	179.3(4)
O1	N20	C4	N18	-5.3(7)	N15	N16	C7	N17	-179.1(4)
O2	N2	C8	N4	-3.2(7)	N15	N16	C7	N19	1.1(7)
O2	N2	C8	N14	175.8(4)	N16	N15	C9	N5	1.6(7)
O3	N13	C6	N10	-172.7(4)	N16	N15	C9	N14	-179.7(4)
O3	N13	C6	N11	7.5(7)	N18	N19	C7	N16	-179.3(4)
O4	N1	C1	N3	5.5(7)	N18	N19	C7	N17	0.9(6)
O4	N1	C1	N6	-172.3(5)	N19	N18	C4	N17	-0.3(6)
O8	N1	C1	N3	-174.2(4)	N19	N18	C4	N20	178.3(4)
O8	N1	C1	N6	8.0(7)	C1	N3	C3	N7	0.9(5)
O9	N13	C6	N10	8.2(7)	C1	N3	C3	N8	179.9(4)
O9	N13	C6	N11	-171.6(4)	C1	N6	N7	C3	-0.2(5)
O10	N2	C8	N4	174.8(4)	C3	N3	C1	N1	-179.1(4)
O10	N2	C8	N14	-6.1(7)	C3	N3	C1	N6	-1.2(6)
O11	N20	C4	N17	-6.1(7)	C3	N8	N9	C5	149.7(4)
O11	N20	C4	N18	175.4(4)	C4	N17	C7	N16	179.2(5)
N4	N5	C9	N14	1.1(6)	C4	N17	C7	N19	-0.9(5)
N4	N5	C9	N15	179.9(4)	C4	N18	N19	C7	-0.3(5)
N5	N4	C8	N2	-180.0(4)	C5	N10	C6	N11	-0.3(5)
N5	N4	C8	N14	0.9(6)	C5	N10	C6	N13	179.9(4)
N6	N7	C3	N3	-0.5(6)	C6	N10	C5	N9	-179.7(4)
N6	N7	C3	N8	-179.4(4)	C6	N10	C5	N12	1.0(5)
N7	N6	C1	N1	178.8(4)	C6	N11	N12	C5	1.2(5)
N7	N6	C1	N3	0.9(6)	C7	N17	C4	N18	0.8(6)
N8	N9	C5	N10	176.5(4)	C7	N17	C4	N20	-177.8(4)
N8	N9	C5	N12	-4.3(7)	C8	N4	N5	C9	-1.1(5)
N9	N8	C3	N3	176.2(4)	C8	N14	C9	N5	-0.5(5)
N9	N8	C3	N7	-5.0(7)	C8	N14	C9	N15	-179.3(5)
N11	N12	C5	N9	179.3(4)	C9	N14	C8	N2	-179.4(4)
N11	N12	C5	N10	-1.5(5)	C9	N14	C8	N4	-0.3(6)
N12	N11	C6	N10	-0.5(5)	C9	N15	N16	C7	-145.0(4)

5.2 Single crystal structure of LX-11

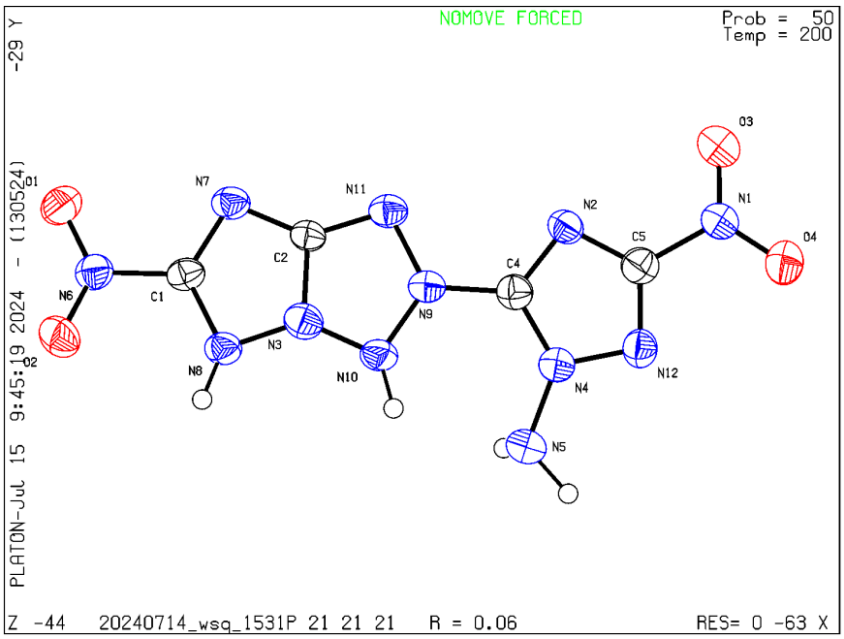

Figure S5 Crystal structures of compound **LX-11**.

Table S9 Crystal data and structure refinement for compound **LX-11**.

Compound	**LX-11**
Formula	$C_4H_4N_{12}O_4$
M_w[g mol^{-1}]	284.19
T[K]	200
Wavelength	1.34139 Å
Crystal system	orthorhombic
Space group	$P2_12_12_1$
a[Å]	5.9463(4)
b[Å]	6.6224(5)
c[Å]	24.2123(18)
α[°]	90
β[°]	90
γ[°]	90
V[Å^3]	953.45(12)
Z	4
$\rho_{calc.}$[g cm^{-3}]	1.980
Absorption coefficient [mm^{-1}]	0.978
F[000]	576.0
Crystal size[mm^3]	0.200 x 0.100 x 0.100
Theta range for data collection [°]	12.054 to 114.098
Index ranges	-7≤h≤7, -7≤k≤8, -29≤I≤30
Reflections collected	9578
Data/restraints/parameters	1940/1/189
Final R index[$I > 2\sigma(I)$]	R_1 = 0.0577, wR_2 = 0.1548
R indices (all data)	R_1 = 0.0721, wR_2 = 0.1689
Goodness-of-fit on F^2	1.058
CCDC	2386022

Table S10 Crystal Atomic coordinates (x 10^4) and equivalent isotropic displacement parameters (Å^{2}x 10^3) for **LX-11** U(eq) is defined as one third of the trace of the orthogonalized U^{ij} tensor.

	x	y	z	U(eq)
O1	464(7)	6177(6)	1118.1(16)	47.3(10)
O2	-2222(6)	4967(6)	1638.0(14)	45.6(10)

O3	12188(7)	7475(6)	4343.8(15)	51.5(11)
O4	11364(7)	5792(7)	5063.0(16)	50.3(11)
N1	10965(7)	6398(7)	4596.5(18)	38.5(10)
N2	8205(7)	6419(6)	3842.2(18)	33.6(10)
N12	7649(7)	4363(7)	4580.6(17)	36.1(10)
N4	5954(7)	4157(6)	4213.8(17)	34.1(9)
N5	4134(9)	2904(8)	4317(2)	44.5(12)
N6	-304(7)	5523(7)	1549.3(18)	36.0(10)
N7	3167(7)	6480(7)	2014.2(18)	33.9(10)
N8	461(7)	4615(7)	2487.6(18)	33.4(10)
N9	4899(7)	5531(6)	3326.5(18)	31.5(9)
N10	2897(7)	4621(7)	3319.1(18)	34.7(10)
N11	5594(7)	6491(6)	2862.3(17)	33.6(10)
C1	1173(8)	5530(7)	2029.8(19)	30.8(10)
C2	3838(8)	6129(7)	2532.9(19)	28.5(10)
N3	2247(7)	5036(7)	2811.0(19)	36.6(10)
C4	6326(8)	5395(7)	3785(2)	32.5(11)
C5	8905(9)	5722(8)	4331(2)	35.5(11)

Table S11 Bond lengths [Å] for compound **LX-11**.

Atom	Atom	Length/Å	Atom	Atom	Length/Å
O1	N6	1.219(5)	N6	C1	1.458(6)
O2	N6	1.217(6)	N7	C1	1.343(6)
O3	N1	1.188(5)	N7	C2	1.338(6)
O4	N1	1.222(6)	N8	C1	1.333(6)
N1	C5	1.454(7)	N8	N3	1.349(6)
N2	C4	1.315(6)	N9	N10	1.335(6)
N2	C5	1.336(7)	N9	N11	1.356(6)
N12	N4	1.351(6)	N9	C4	1.401(6)
N12	C5	1.317(7)	N10	N3	1.318(6)
N4	N5	1.386(6)	N11	C2	1.336(6)
N4	C4	1.340(6)	C2	N3	1.368(6)

Table S12 Bond angles [°] for compound **LX-11**.

Atom	Atom	Atom	Angle/°	Atom	Atom	Atom	Angle/°
O3	N1	O4	123.7(5)	C2	N11	N9	99.9(4)
O3	N1	C5	118.2(4)	N7	C1	N6	120.7(4)
O4	N1	C5	118.1(4)	N8	C1	N6	118.1(4)
C4	N2	C5	100.3(4)	N8	C1	N7	121.1(4)
C5	N12	N4	101.0(4)	N7	C2	N3	110.3(4)
N12	N4	N5	121.7(4)	N11	C2	N7	139.7(5)
C4	N4	N12	108.9(4)	N11	C2	N3	110.0(4)
C4	N4	N5	129.4(4)	N8	N3	C2	111.6(4)
O1	N6	C1	117.2(4)	N10	N3	N8	136.8(4)
O2	N6	O1	127.5(5)	N10	N3	C2	111.5(4)
O2	N6	C1	115.1(4)	N2	C4	N4	112.0(4)
C2	N7	C1	99.0(4)	N2	C4	N9	124.4(4)
C1	N8	N3	98.0(4)	N4	C4	N9	123.6(4)
N10	N9	N11	118.2(4)	N2	C5	N1	123.2(5)
N10	N9	C4	121.4(4)	N12	C5	N1	119.0(4)
N11	N9	C4	120.2(4)	N12	C5	N2	117.8(5)

Table S13 Torsion Angles [°] for compound **LX-11**.

A	B	C	D	Angle/°	A	B	C	D	Angle/°
O1	N6	C1	N7	9.3(7)	N10	N9	C4	N4	9.1(7)
O1	N6	C1	N8	-172.4(4)	N11	N9	N10	N3	-0.3(5)
O2	N6	C1	N7	-166.5(4)	N11	N9	C4	N2	11.7(7)
O2	N6	C1	N8	11.7(6)	N11	N9	C4	N4	-166.5(4)
O3	N1	C5	N2	-7.4(7)	N11	C2	N3	N8	-179.0(4)

O3	N1	C5	N12	172.9(5)	N11	C2	N3	N10	-0.9(6)
O4	N1	C5	N2	174.2(5)	C1	N7	C2	N11	178.7(6)
O4	N1	C5	N12	-5.6(7)	C1	N7	C2	N3	-0.1(5)
N12	N4	C4	N2	0.6(6)	C1	N8	N3	N10	-177.5(6)
N12	N4	C4	N9	179.0(4)	C1	N8	N3	C2	-0.1(5)
N4	N12	C5	N1	179.8(4)	C2	N7	C1	N6	178.3(4)
N4	N12	C5	N2	0.1(6)	C2	N7	C1	N8	0.1(6)
N5	N4	C4	N2	177.2(5)	N3	N8	C1	N6	-178.3(4)
N5	N4	C4	N9	-4.4(8)	N3	N8	C1	N7	0.0(6)
N7	C2	N3	N8	0.1(6)	C4	N2	C5	N1	-179.4(5)
N7	C2	N3	N10	178.2(4)	C4	N2	C5	N12	0.3(6)
N9	N10	N3	N8	178.1(5)	C4	N9	N10	N3	-176.1(4)
N9	N10	N3	C2	0.7(5)	C4	N9	N11	C2	175.6(4)
N9	N11	C2	N7	-178.2(6)	C5	N2	C4	N4	-0.5(5)
N9	N11	C2	N3	0.6(5)	C5	N2	C4	N9	-178.9(5)
N10	N9	N11	C2	-0.2(5)	C5	N12	N4	N5	-177.3(5)
N10	N9	C4	N2	-172.7(4)	C5	N12	N4	C4	-0.4(5)

5.3 Single crystal structure of 6

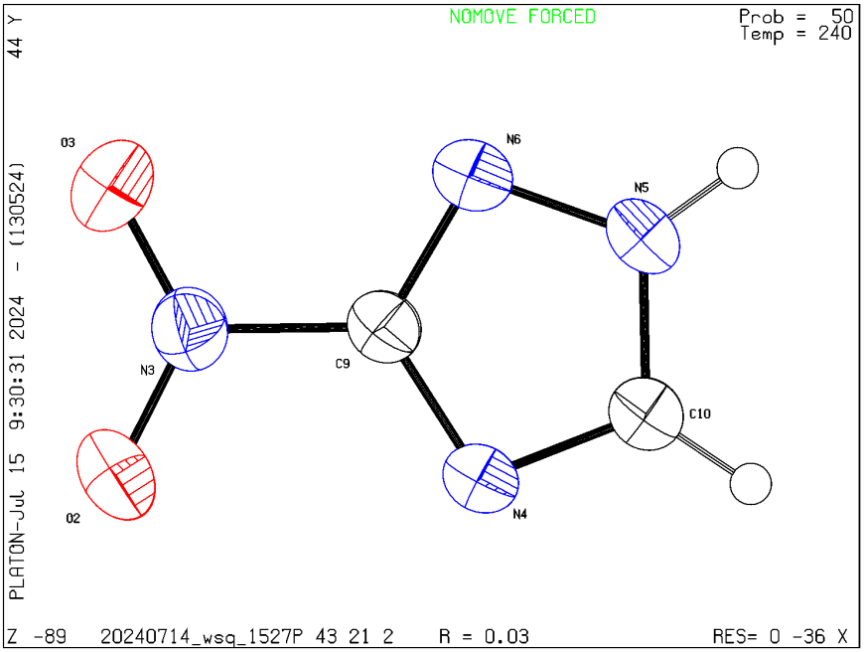

Figure S6 Crystal structures of compound **6**.

Table S14 Crystal data and structure refinement for compound **6**.

Compound	**6**
Formula	$C_2H_2N_4O_2$
M_w[g mol^{-1}]	114.08
T[K]	240
Wavelength	1.34139 Å
Crystal system	tetragonal
Space group	$P4_32_12$
a[Å]	6.8684(2)
b[Å]	6.8684(2)
c[Å]	19.1626(10)
α[°]	90
β[°]	90
γ[°]	90
V[Å^3]	903.99(7)

Z	8
$\rho_{calc.}$[g cm^{-3}]	1.676
Absorption coefficient [mm^{-1}]	0.833
F[000]	464.0
Crystal size[mm^3]	0.200 x 0.160 x 0.120
Theta range for data collection [°]	11.908 to 114.282
Index ranges	-8≤h≤7, -8≤k≤7, -23≤I≤23
Reflections collected	6988
Data/restraints/parameters	931/0/73
Final *R* index[$I > 2\sigma(I)$]	R_1 = 0.0277, wR_2 = 0.0736
R indices (all data)	R_1 = 0.0287, wR_2 = 0.0746
Goodness-of-fit on F^2	1.080
CCDC	2386020

Table S15 Crystal Atomic coordinates (x 10^4) and equivalent isotropic displacement parameters (Å^{2}x 10^3) for **6** U(eq) is defined as one third of the trace of the orthogonalized U^{ij} tensor.

	x	y	z	U(eq)
O2	3269.5(18)	5988.4(17)	6659.6(6)	45.0(3)
O3	5461(2)	4760(2)	5985.9(7)	71.0(5)
N3	4377(2)	4692(2)	6486.6(7)	39.5(3)
N4	3248(2)	2730.1(19)	7467.2(7)	36.4(4)
N5	5201(2)	287(2)	7300.2(7)	42.4(4)
N6	5649(2)	1542(2)	6783.5(7)	44.8(4)
C9	4426(2)	2953(2)	6915.5(8)	32.9(3)
C10	3794(3)	995(3)	7696.3(8)	39.6(4)

Table S16 Bond lengths [Å] for compound **6**.

Atom	Atom	Length/Å	Atom	Atom	Length/Å
O2	N3	1.2172(17)	N4	C10	1.324(2)
O3	N3	1.2151(18)	N5	N6	1.3488(19)
N3	C9	1.4502(19)	N5	C10	1.322(2)
N4	C9	1.340(2)	N6	C9	1.307(2)

Table S17 Bond angles [°] for compound **6**.

Atom	Atom	Atom	Angle/°	Atom	Atom	Atom	Angle/°
O2	N3	C9	117.55(13)	C9	N6	N5	100.70(13)
O3	N3	O2	124.74(14)	N4	C9	N3	121.83(13)
O3	N3	C9	117.70(13)	N6	C9	N3	121.05(14)
C10	N4	C9	101.17(13)	N6	C9	N4	117.12(14)
C10	N5	N6	110.66(13)	N5	C10	N4	110.36(13)

Table S18 Torsion Angles [°] for compound **LX-11**.

A	B	C	D	Angle/°	A	B	C	D	Angle/°
O2	N3	C9	N4	2.6(2)	N6	N5	C10	N4	-0.1(2)
O2	N3	C9	N6	-176.48(16)	C9	N4	C10	N5	0.31(18)
O3	N3	C9	N4	-178.27(16)	C10	N4	C9	N3	-179.53(15)
O3	N3	C9	N6	2.7(2)	C10	N4	C9	N6	-0.4(2)
N5	N6	C9	N3	179.46(14)	C10	N5	N6	C9	-0.11(19)
N5	N6	C9	N4	0.3(2)					

6. Other Characterization Plots for LX-11

6.1 The optimized Cartesian coordinates of LX-11

Table S19 The optimized Cartesian coordinates of **LX-11**.

	x(Bohr)	y(Bohr)	z(Bohr)

1(O)	0.521391	7.730220	5.115824
2(N)	9.219859	8.033072	17.579839
3(N)	8.595088	5.460086	20.958359
4(N)	6.690437	5.202287	19.280080
5(N)	4.645326	3.634217	19.752268
6(N)	3.558719	8.109410	9.215895
7(N)	0.518020	5.775452	11.381918
8(N)	5.504947	6.921782	15.220273
9(N)	3.255324	5.782961	15.186415
10(H)	2.477350	4.925691	16.380656
11(N)	6.285910	8.123176	13.096344
12(C)	1.318086	6.920531	9.287272
13(C)	4.312714	7.670151	11.589187
14(N)	2.524927	6.302313	12.861623
15(C)	7.108449	6.751585	17.318122
16(C)	10.006440	7.160810	19.816324
17(H)	4.786910	2.653079	18.759392
18(H)	4.595883	2.728166	21.413160
19(O)	-2.496834	6.215963	7.494606
20(N)	-0.341601	6.911771	7.088763
21(H)	-0.881825	4.936141	11.700004
22(O)	13.695507	9.354605	19.874890
23(O)	12.769589	7.248411	23.165562
24(N)	12.321237	8.006791	21.031109

6.2 The PXRD of LX-11

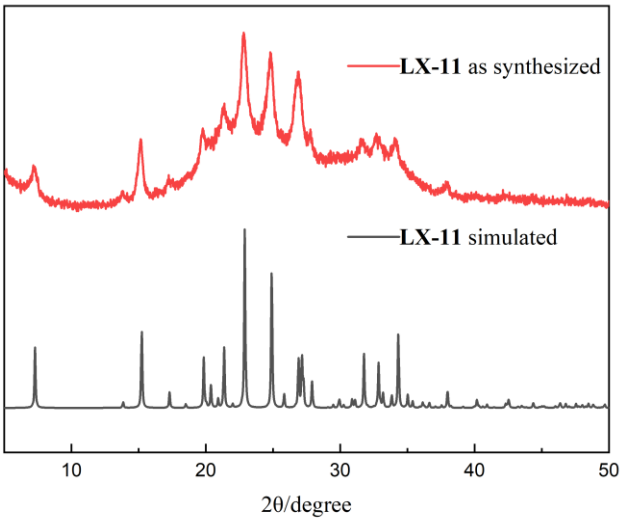

Figure S7 PXRD pattern of **LX-11** at 298 K and the simulated PXRD pattern of **LX-11** single crystal at 200K.

6.3 The RDG scatter plot of LX-11

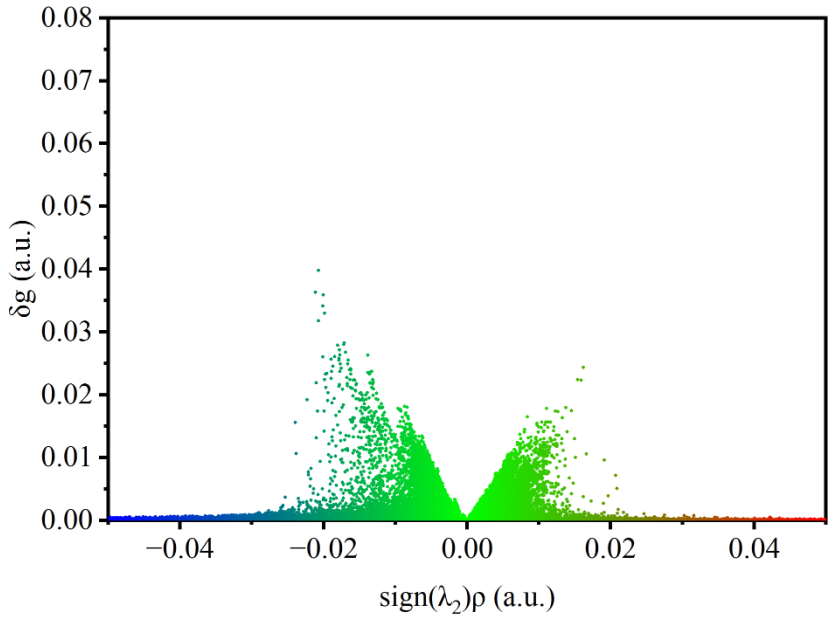

Figure S8 The RDG scatter plot of **LX-11**.

6.4 The RDG scatter plot of LX-11

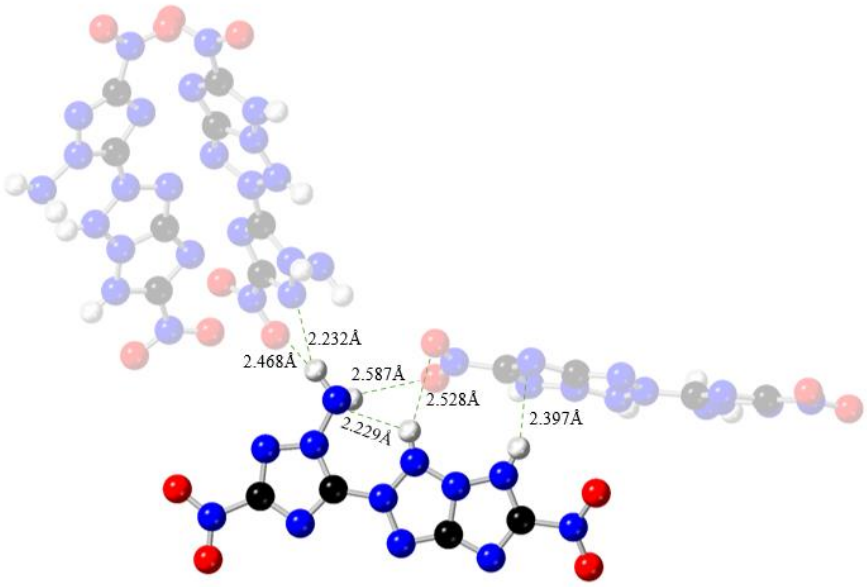

Figure S9 The hydrogen bond data of the single crystal structure of **LX-11**.

7. Explosives with detonation velocities above 9000 m·s^{-1}

Table S20 Physical properties and detonation performance of 173 explosives.

Comp.	T_d / °C	ρ g cm^{-3}	N+O / %	ΔH_f / kJ g^{-1}	D_{v} / m s^{-1}	IS / J	Ref.

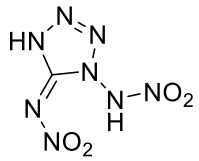	110	1.93	92.62	2.56	9967	1	[4]
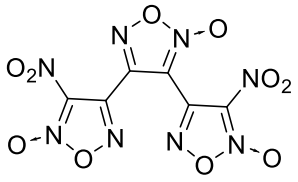	131	1.98	79.05	1.94	9867	3	[5]
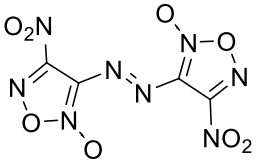	124	1.98	83.33	1.12	9778	1	[6]
	146	1.97	81.52	1.70	9750	4	[7]
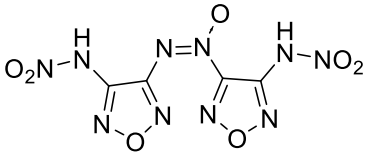	90	1.96	83.43	2.42	9746	2	[8]
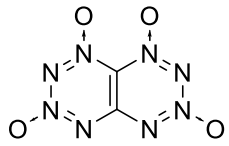	183	1.98	88.00	4.31	9710	--	[9]
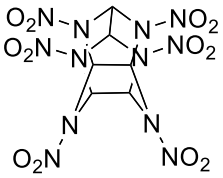	195	2.03	82.17	0.91	9706	4	[10]
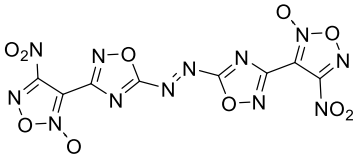	180	1.92	77.35	2.80	9666	12	[10]
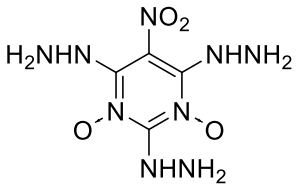	214	1.92	76.89	1.47	9638	>40	[11]

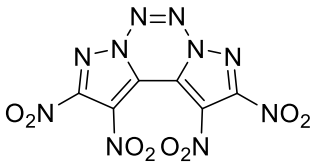	233	1.96	78.81	2.23	9631	10	[12]
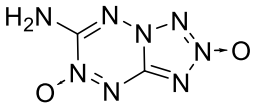	150	1.93	84.69	3.39	9600	6	[13]
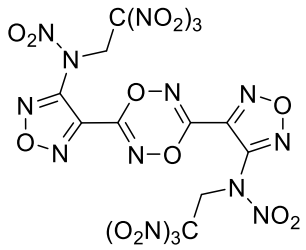	119	1.95	81.42	1.79	9600	4	[14]
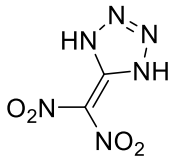	92	1.87	85.04	3.85	9594	3	[15]
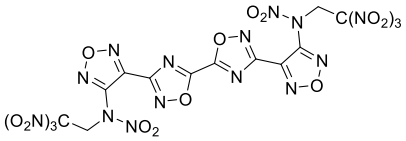	152	1.93	79.43	1.90	9550	5	[16]
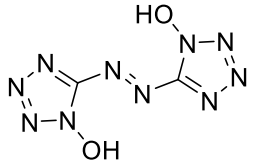	170	1.90	86.85	4.46	9548	<1	[17]
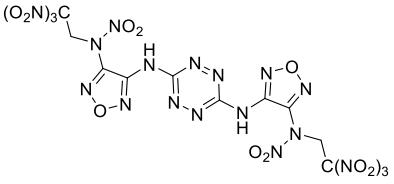	144	1.92	81.83	2.15	9548	10	[18]
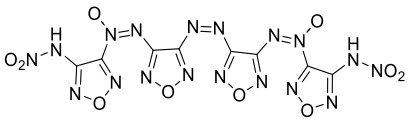	120	1.88	80.78	3.18	9541	2	[19]
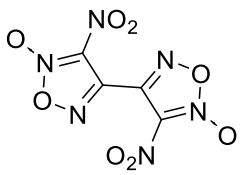	140	1.97	81.52	1.38	9525	-	[20]

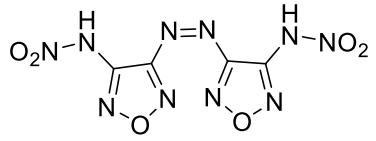	100	1.89	82.50	2.86	9517	2	[8]
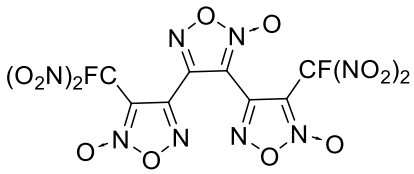	116	2.00	73.08	0.78	9509	5	[21]
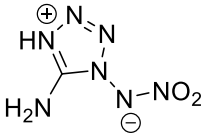	113	1.83	89.64	3.60	9508	-	[22]
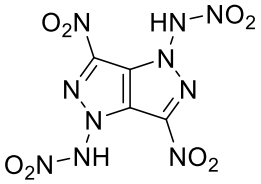	128	1.93	84.26	1.87	9507	2	[23]
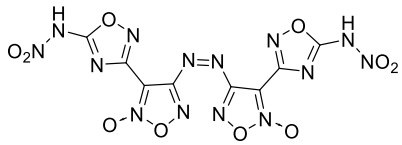	126	1.92	78.41	2.73	9505	4	[24]
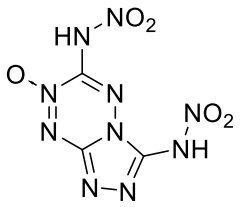	114	1.93	85.26	2.30	9503	1	[25]
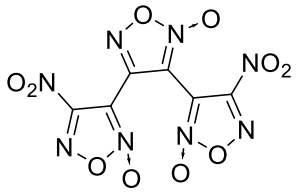	147	1.91	79.05	1.68	9503	3	[5]
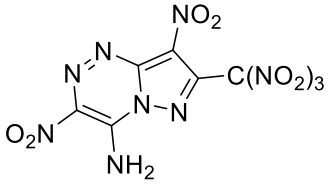	205	1.95	80.20	1.69	9492	12	[26]
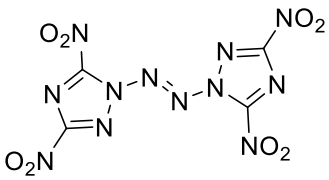	262	1.93	86.03	2.83	9490	10	[27]

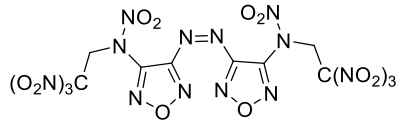	159	1.87	83.65	0.15	9486	4	[28]
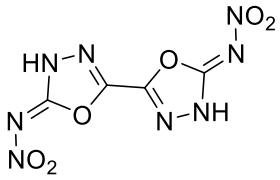	210	1.99	80.60	0.62	9481	5	[29]
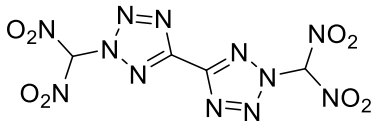	91	1.88	85.54	2.42	9480	4	[30]
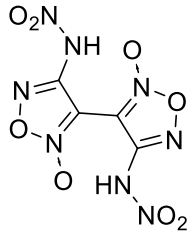	91	1.94	82.75	1.48	9472	2	[31]
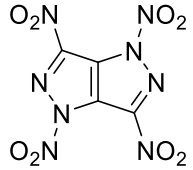	145	1.95	83.33	1.92	9460	3	[23]
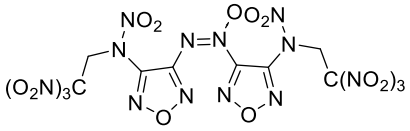	145	1.92	84.06	1.53	9458	3	[32]
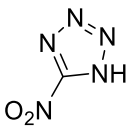	130	1.90	88.68	2.44	9457	<1	[33]
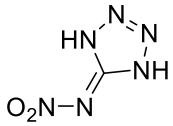	122	1.87	89.21	2.48	9450	2	[34]
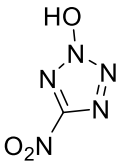	120	1.94	90.06	2.35	9447	--	[35]

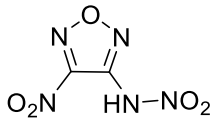	65	1.94	85.71	1.51	9438	4	[36]
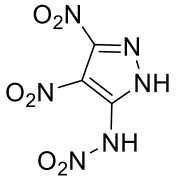	135	1.97	82.56	0.80	9430	4	[37]
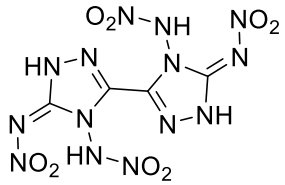	137	1.91	86.16	1.88	9421	5	[38]
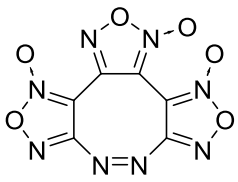	161	1.90	74.27	3.22	9417	19	[39]
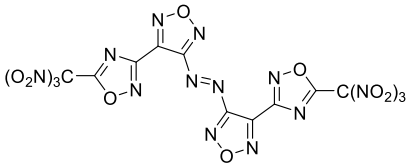	119	1.93	79.99	1.54	9411	3	[40]
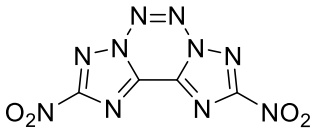	138	1.91	80.94	3.12	9400	5	[41]
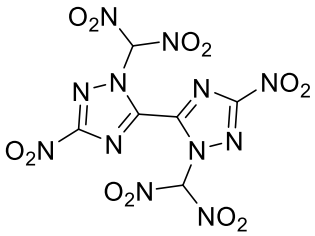	166	1.95	82.94	0.90	9394	4	[42]
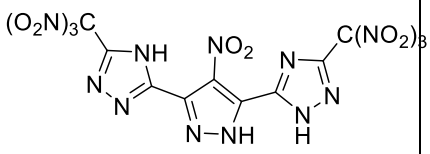	155	1.90	79.62	1.71	9390	13	[43]
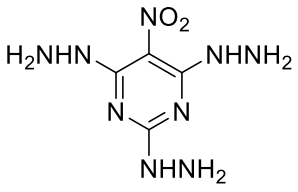	207	1.88	73.46	1.24	9386	35	[11]

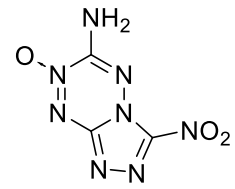	220	1.86	80.79	3.76	9384	25	[44]
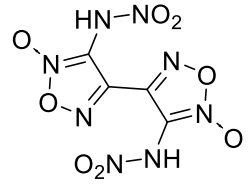	75	1.91	82.75	1.59	9381	3	[31]
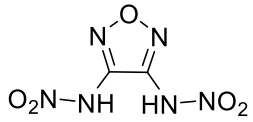	99	1.90	86.31	1.51	9376	<1	[45]
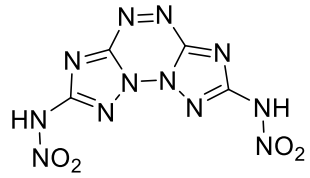	185	2.00	82.25	3.04	9370	8	[46]
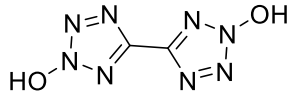	165	1.95	84.69	3.29	9364	3	[47]
	181	1.84	82.85	4.09	9363	8	[11]
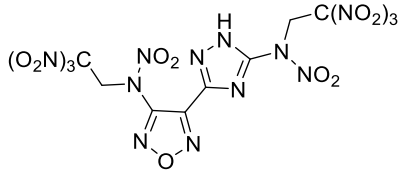	92	1.93	82.67	0.77	9355	3	[48]
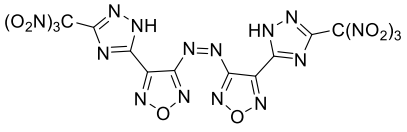	144	1.90	79.58	2.09	9354	5	[49]
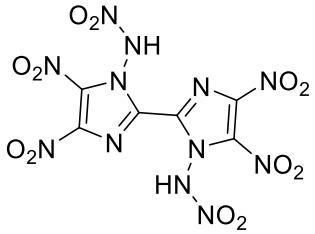	116	1.94	82.94	1.10	9350	3	[50]

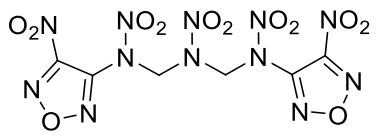	150	1.90	82.56	1.38	9334	2	[36]
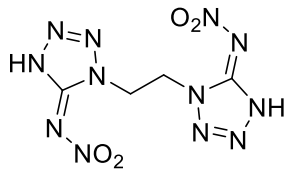	194	1.86	81.10	3.36	9329	10	[51]
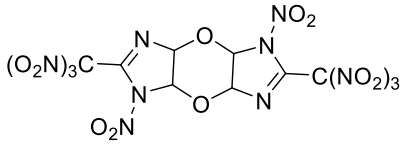	127	1.91	82.00	0.79	9325	--	[52]
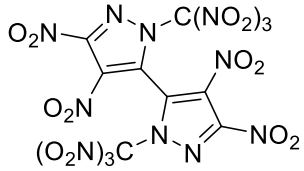	125	2.02	84.30	0.85	9320	9	[53]
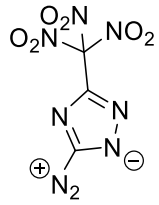	127	1.89	85.24	2.14	9317	<1	[54]
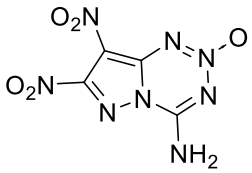	295	1.96	79.32	1.84	9317	18	[55]
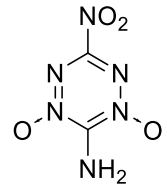	110	1.92	85.04	1.29	9316	3	[56]
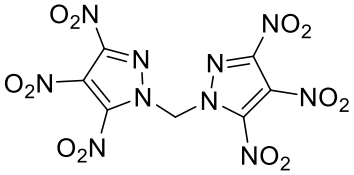	205	1.93	79.41	0.91	9304	4	[57]

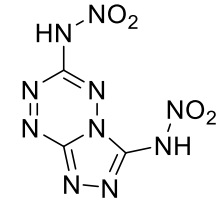	138	1.91	84.28	3.06	9301	3	[58]
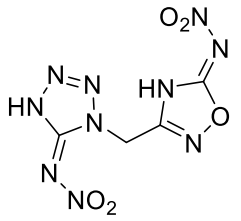	175	1.88	80.86	2.82	9297	12	[59]
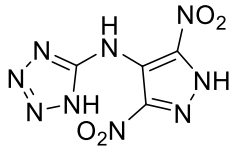	279	1.86	78.82	2.02	9289	35	[60]
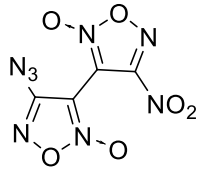	113	1.83	81.24	3.00	9280	2	[7]
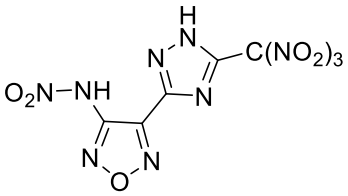	67	1.89	82.70	1.59	9278	4	[61]
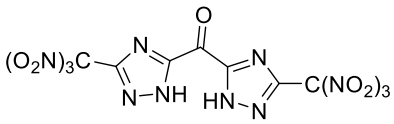	150	1.93	81.37	0.63	9275	13	[62]
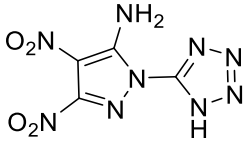	222	1.85	78.82	2.96	9261	25	[63]
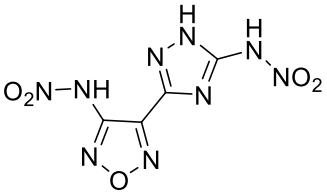	129	1.92	80.14	2.13	9258	18	[64]
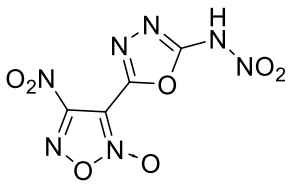	86	1.88	81.06	1.68	9258	8	[65]

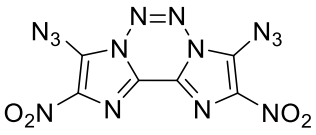	111	1.89	79.31	3.97	9256	2	[66]
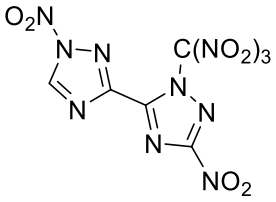	136	1.90	83.72	1.36	9254	11	[67]
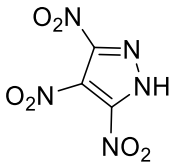	220	1.87	81.76	0.17	9253	17	[68]
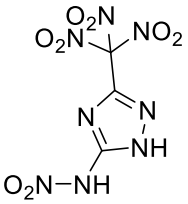	125	1.91	86.31	0.97	9250	2	[69]
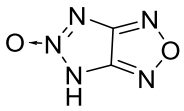	89	1.93	80.30	0.92	9250	3	[70]
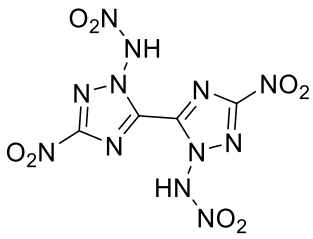	121	1.88	85.54	1.71	9243	3	[71]
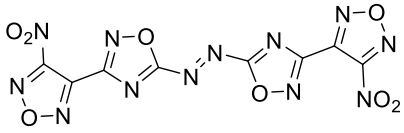	256	1.92	75.50	2.46	9240	18	[72]
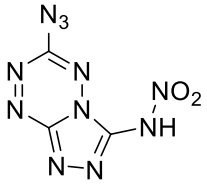	150	1.85	83.40	4.27	9236	1	[73]
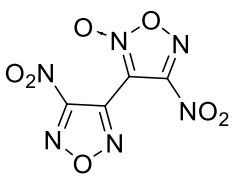	140	1.93	80.31	1.71	9230	3	[74]

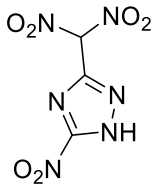	87	1.91	82.56	0.38	9229	10	[75]
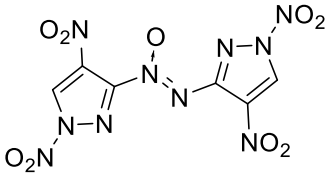	161	1.83	79.31	2.42	9228	7	[76]
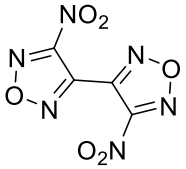	85	1.85	78.94	1.81	9227	--	[31]
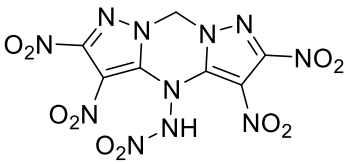	117	1.94	78.29	1.30	9226	3	[77]
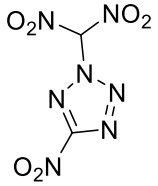	109	1.97	88.58	1.42	9220	5	[78]
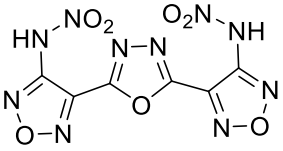	67	1.91	77.29	2.18	9211	--	[79]
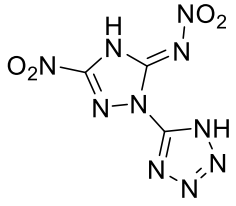	129	1.83	84.28	2.96	9209	15	[80]
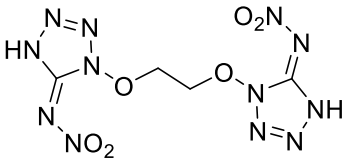	134	1.81	83.00	3.47	9200	2	[81]
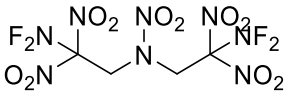	154	2.03	68.00	-0.15	9200	3	[82]

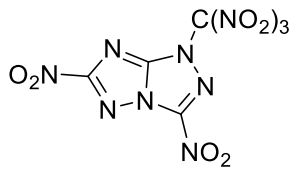	168	1.97	86.20	1.25	9199	12	[83]
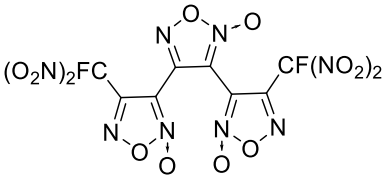	136	1.91	73.08	0.77	9196	7	[21]
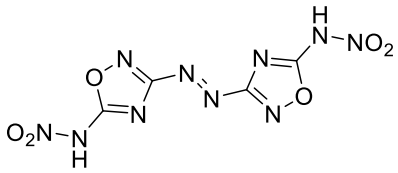	140	1.90	82.50	1.70	9190	2	[84]
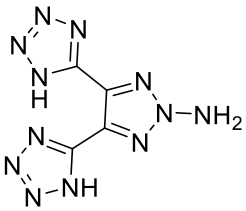	303	1.86	76.35	4.63	9185	>40	[85]
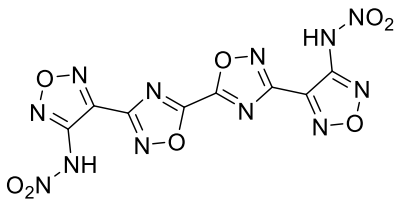	101	1.92	75.11	2.40	9185	16	[16]
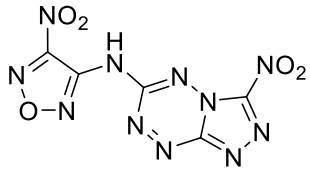	184	1.86	79.31	3.16	9182	>40	[86]
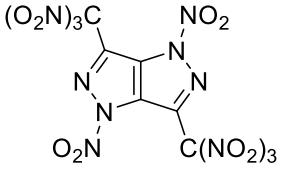	160	1.99	85.48	1.17	9182	7	[87]
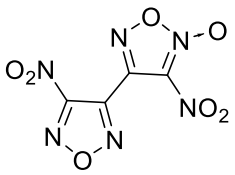	146	1.92	80.31	1.71	9180	3	[74]

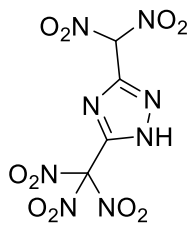	143	1.97	84.46	0.18	9180	6	[88]
	284	1.95	73.24	-0.04	9169	>60	[89]
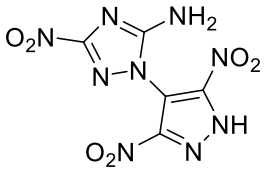	270	1.84	77.88	1.54	9167	9	[90]
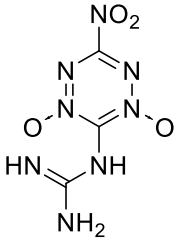	134	1.91	81.46	1.50	9157	20	[56]
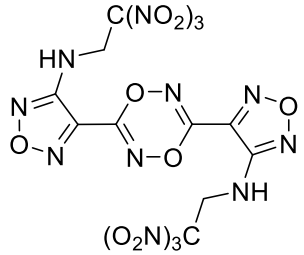	203	1.94	78.18	1.24	9156	16	[14]
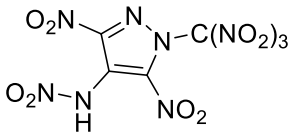	68	1.99	86.64	0.84	9155	2	[91]
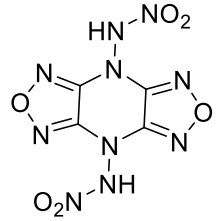	74	1.80	82.50	2.62	9153	1	[92]
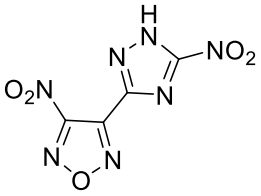	191	1.86	78.41	1.78	9152	23	[48]

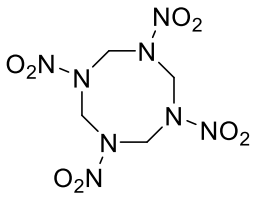	279	1.91	81.06	0.25	9144	7	[92]
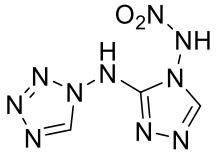	177	1.78	81.11	4.36	9141	18	[93]
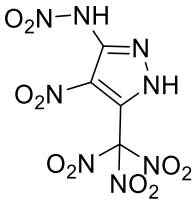	124	1.90	84.45	0.99	9124	5	[94]
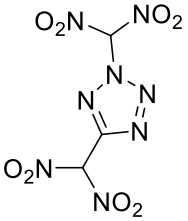	88	1.92	86.31	0.89	9123	3	[95]
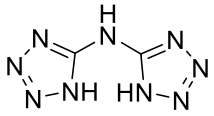	250	1.86	82.34	4.14	9120	>30	[96]
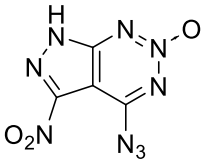	203	1.85	78.01	3.47	9120	18	[97]
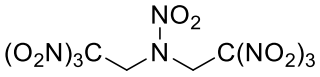	98	1.96	86.58	-0.07	9120	4	[53]
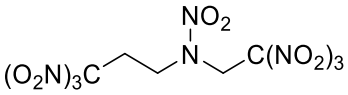	153	1.89	83.56	-0.17	9119	7	[98]
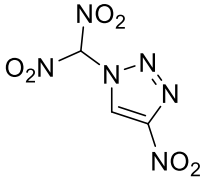	105	1.88	82.56	0.89	9115	7	[99]
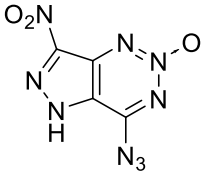	160	1.86	78.01	3.34	9111	60	[100]

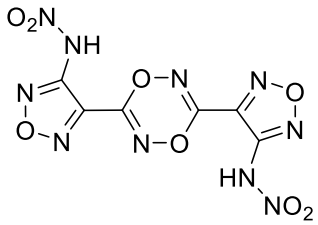	106	1.93	78.35	2.48	9109	5	[14]
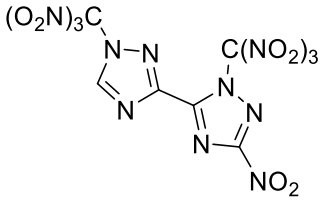	152	1.92	84.75	0.95	9107	5	[67]
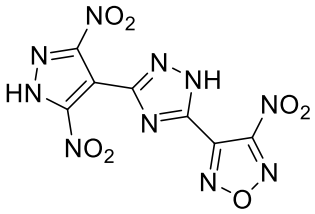	302	1.89	74.54	2.31	9103	35	[101]
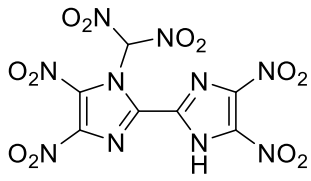	142	1.92	79.41	0.50	9102	9	[102]
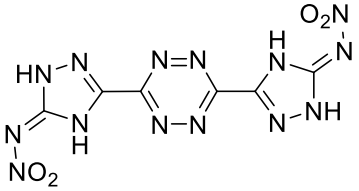	162	1.88	77.37	3.95	9100	20	[103]
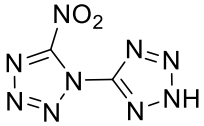	122	1.77	86.33	3.59	9099	1	[104]
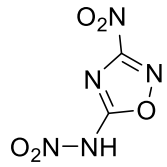	219	1.88	85.71	1.30	9095	15	[105]
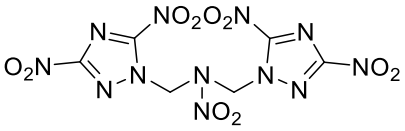	209	1.90	81.17	1.10	9089	<1	[106]

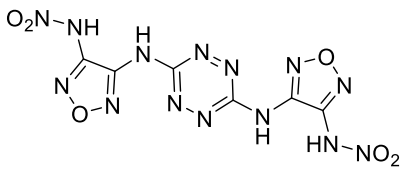	149	1.85	79.33	3.00	9087	16	[18]
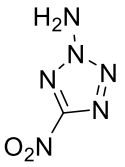	140	1.79	89.21	2.89	9087	<1	[107]
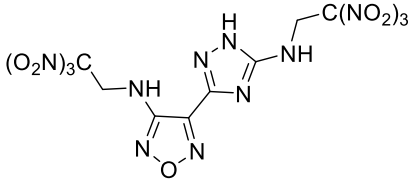	168	1.91	79.09	1.01	9087	8	[48]
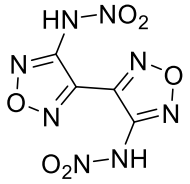	80	1.94	80.60	2.04	9086	2	[31]
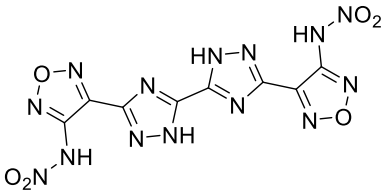	112	1.94	74.48	2.52	9083	16	[108]
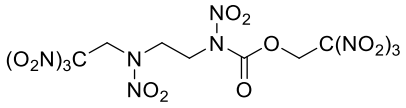	157	1.89	82.29	-0.56	9083	10	[109]
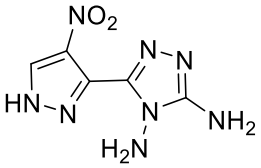	226	1.87	68.55	2.26	9075	>80	[110]
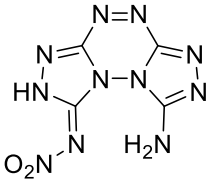	166	1.88	78.46	2.41	9073	>40	[111]
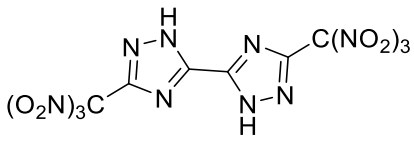	148	1.89	82.94	0.76	9073	23	[54]

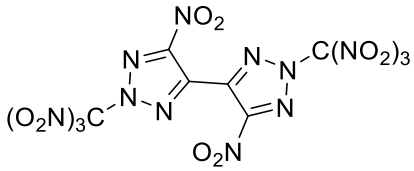	195	1.92	86.25	0.90	9070	5	[53]
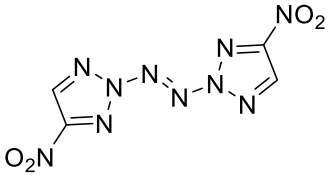	227	1.84	80.30	3.31	9068	5	[112]
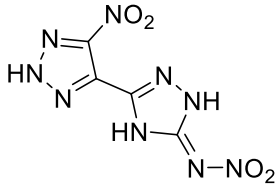	168	1.88	78.82	2.46	9067	16	[113]
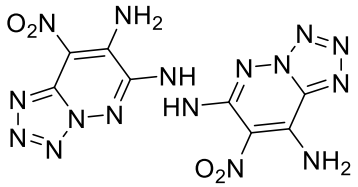	292	1.84	73.83	2.76	9064	16	[114]
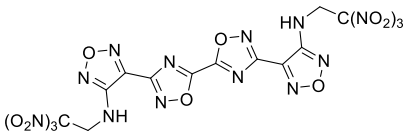	188	1.90	76.17	1.43	9062	11	[16]
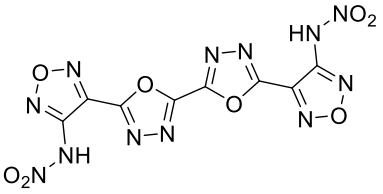	90	1.92	75.11	2.01	9058	7	[115]
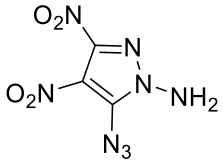	121	1.82	82.23	2.56	9053	2	[116]
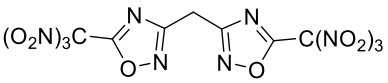	117	1.91	80.88	0.39	9053	13	[117]
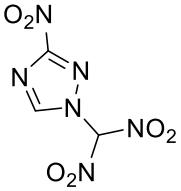	131	1.85	82.56	1.43	9050	7	[78]

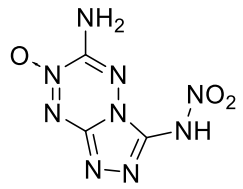	182	1.88	81.67	2.28	9047	10	[73]
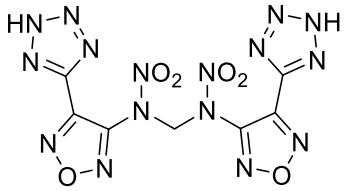	154	1.83	78.42	3.50	9043	16	[118]
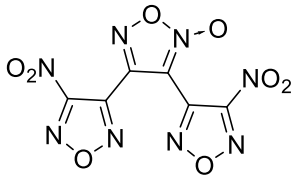	231	1.87	76.91	1.93	9043	14	[119]
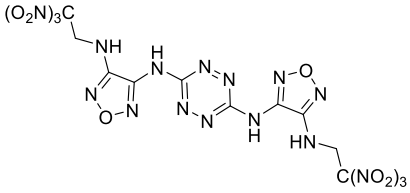	204	1.86	78.79	2.12	9042	21	[18]
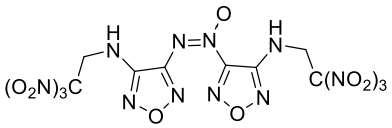	190	1.84	81.02	1.41	9041	8	[32]
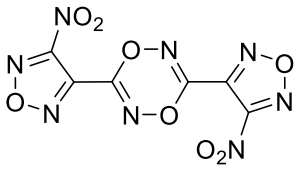	148	1.87	76.10	1.85	9040	2	[120]
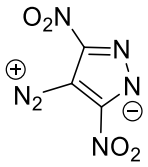	154	1.81	80.43	2.22	9038	3	[121]
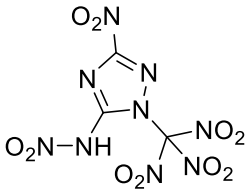	121	1.97	88.54	-0.69	9033	4	[122]
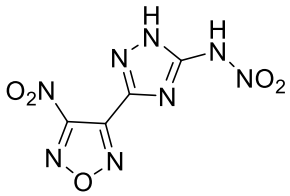	163	1.85	79.32	2.17	9025	20	[64]

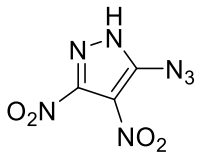	141	1.79	81.39	2.81	9023	8	[123]
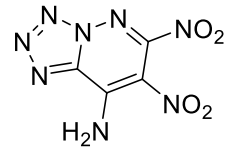	202	1.89	77.86	2.08	9021	18	[124]
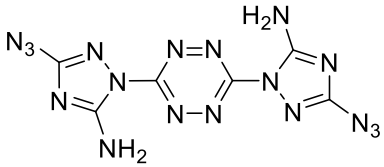	186	1.91	76.82	4.44	9017	6	[125]
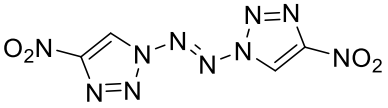	160	1.82	80.30	3.41	9014	<1	[112]
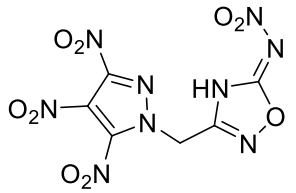	170	1.84	78.24	1.39	9014	2	[126]
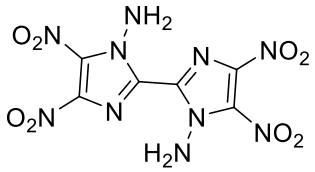	217	1.93	77.89	0.90	9012	15	[50]
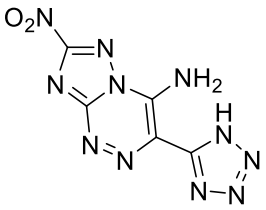	181	1.87	74.68	2.90	9010	35	[127]
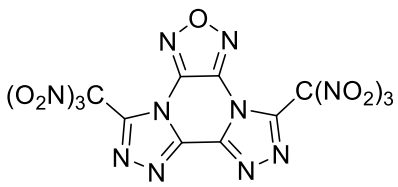	128	1.89	80.79	1.41	9010	11	[128]
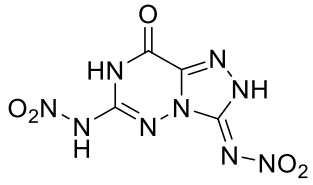	150	1.95	80.14	1.11	9010	4	[129]

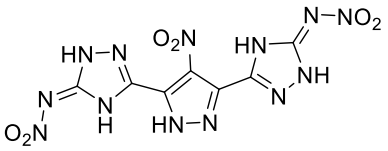	134	1.92	75.73	2.16	9008	20	[115]
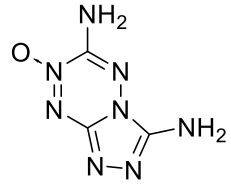	196	1.82	76.17	2.13	9008	>40	[44]
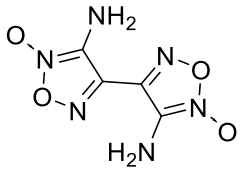	160	1.86	73.98	2.12	9007	6	[20]
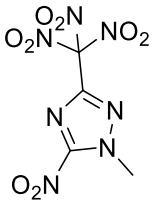	153	1.88	81.57	0.34	9006	13	[75]
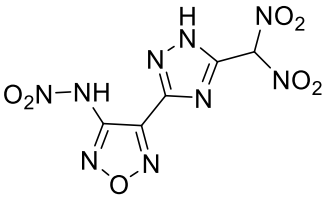	91	1.85	79.05	1.79	9005	9	[61]
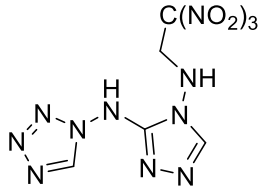	182	1.77	79.98	3.31	9004	22	[93]
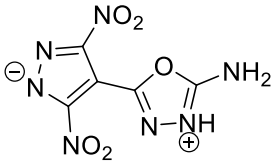	272	1.94	73.84	1.62	9003	40	[130]
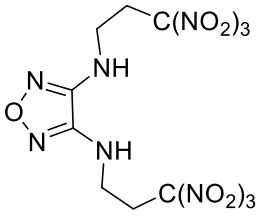	160	1.83	76.63	0.59	8998	7	[131]

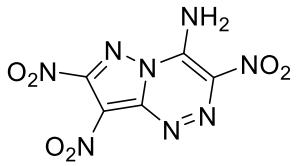	246	1.95	77.02	0.33	8998	14	[132]
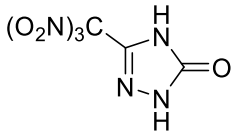	80	1.90	83.74	-0.28	8997	10	[133]
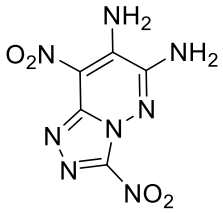	234	1.93	73.31	1.45	8994	20	[134]
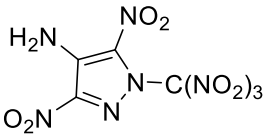	113	1.90	84.46	0.45	8994	15	[135]
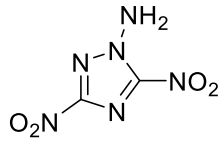	165	1.89	85.04	1.57	8981	30	[107]

8. References

[1] M. J. Frisch, G. W. Trucks, H. B. Schlegel, G. E. Scuseria, M. A. Robb, J. R. Cheeseman, G. Scalmani, V. Barone, B. Mennucci, G. A. Petersson, H. Nakatsuji, M. Caricato, X. Li, H. P. Hratchian, A. F. Izmaylov, J. Bloino, G. Zheng, J. L. Sonnenberg, M. Hada, M. Ehara, K. Toyota, R. Fukuda, J. Hasegawa, M. Ishida, T. Nakajima, Y. Honda, O. Kitao, H. Nakai, T. Vreven, J. A. Montgomery, Jr., J. E. Peralta, F. Ogliaro, M. Bearpark, J. J. Heyd, E. Brothers, K. N. Kudin, V. N. Staroverov, R. Kobayashi, J. Normand, K. Raghavachari, A. Rendell, J. C. Burant, S. S. Iyengar, J. Tomasi, M. Cossi, N. Rega, J. M. Millam, M. Klene, J. E. Knox, J. B. Cross, V. Bakken, C. Adamo, J. Jaramillo, R. Gomperts, R. E. Stratmann, O. Yazyev, A . J. Austin, R. Cammi, C. Pomelli, J. W. Ochterski, R. L. Martin, K. Morokuma, V. G. Zakrzewski, G. A. Voth, P. Salvador, J. J. Dannenberg, S. Dapprich, A. D. Daniels, Ö. Farkas, J. B. Foresman, J. V. Ortiz, J. Cioslowski, D. J. Fox, Gaussian 09, Revision B.01, Gaussian, Inc., Wallingford CT, 2009.

[2] A. D. Becke, *J. Chem. Phys.* **1993**, *98*, 5648-5652.

[3] P. J. Stephens, F. J. Devlin, C. F. Chabalowski, M. J. Frisch, *J. Phys. Chem.* **1994**, *98*, 11623.

[4] D. Fischer, T. M. Klapötke, J. Stierstorfer, *Angew. Chem. Int. Ed.* **2015**, *54*, 10299.

[5] L. Zhai, F. Bi, Y. Luo, N. Wang, J. Zhang, B. Wang, *Sci. Rep.* **2019**, *9*, 4321.

[6] T. Guo, M. Liu, X.-C. Huang, Z. Wang, S. Qiu, Z. Ge, Z. Meng, *J. Anal. Appl. Pyrol.* **2017**, *128*, 451.

[7] A. A. Larin, A. V. Shaferov, M. A. Epishina, I. N. Melnikov, N. V. Muravyev, I. V. Ananyev, L. L. Fershtat, N. N. Makhova, *ACS Appl. Energy Mater.* **2020**, *3*, 7764.

[8] J. Zhang, J. M. Shreeve, *J. Phys. Chem. C* **2015**, *119*, 12887.

[9] M. S. Klenov, A. A. Guskov, O. V. Anikin, A. M. Churakov, Y. A. Strelenko, I. V. Fedyanin, K. A. Lyssenko, V. A. Tartakovsky, *Angew. Chem. Int. Ed.* **2016**, *55*, 11472.
[10] H. Xiong, G. Cheng, Z. Zhang, H. Yang, *New J. Chem.* **2019**, *43*, 7784.
[11] A. K. Yadav, V. D. Ghule, S. Dharavath, *J. Mater. Chem. A* 2022, *10*, 12702.
[12] Y. Tang, D. Kumar, J. M. Shreeve, *J. Am. Chem. Soc.* **2017**, *139*, 13684.
[13] D. E. Chavez, D. A. Parrish, L. Mitchell, G. H. Imler, *Angew. Chem. Int. Ed.* **2017**, *56*, 3575.
[14] Q. Yu, G. Cheng, X. Ju, C. Lu, Q. Lin, H. Yang, *Dalton Trans.* **2017**, *46*, 14301
[15] T. M. Klapötke, F. X. Steemann, *Propellants Explos. Pyrotech.* **2010**, *35*, 114.
[16] B. Wang, H. Xiong, G. Cheng, H. Yang, *ChemPlusChem* **2018**, *83*, 439.
[17] D. Fischer, T. M. Klapötke, D. G. Piercey, J. Stierstorfer, *Chem. Eur. J.* **2013**, *19*, 4602.
[18] Q. Yu, H. Yang, G. H. Imler, D. A. Parrish, G. Cheng, J. M. Shreeve, *ACS Appl. Mater. Interfaces* **2020**, *12*, 31522.
[19] Y. Liu, J. Zhang, K. Wang, J. Li, Q. Zhang, J. M. Shreeve, *Angew. Chem. Int. Ed.* **2016**, *55*, 11548.
[20] D. Fischer, T. M. Klapötke, J. Stierstorfer, *Eur. J. Inorg. Chem.* **2014**, *34*, 5808.
[21] L. Zhai, F. Bi, Y. Luo, L. Sun, H. Huo, J. Zhang, J. Zhang, B. Wang, S. Chen, *Chem. Eng. J.* **2020**, *391*, 123573.
[22] L. Liu, C. He, C. Li, Z. Li, *J. Chem. Crystallogr* **2012**, *42*, 816.
[23] P. Yin, J. Zhang, L. A. Mitchell, D. A. Parrish, J. M. Shreeve, *Angew. Chem. Int. Ed.* **2016**, *55*, 12895.
[24] H. Xiong, H. Yang, C. Lei, P. Yang, W. Hu, G. Cheng, *Dalton Trans.* **2019**, *48*, 14705.
[25] L. Hu, H, Gao, J. M. Shreeve, *J. Mater. Chem. A* **2020**, *8*, 17411.
[26] M. Zhang, L. Zhang, M. Zhu, K. Qin, Q. Lin, J. Mol. Struct. 2024, 1301, 137369.
[27] Y. Li, B. Wang, P. Chang, J. Hu, T. Chen, Y. Wang, B. Wang, *RSC Adv.* **2018**, *8*, 13755.
[28] Q. Yu, Z. Wang, B. Wu, H. Yang, X. Ju, C. Lu, G. Cheng, *J. Mater. Chem. A* **2015**, *3*, 8156.
[29] W. Zhang, J. Zhang, M. Deng, X. Qi, F. Nie, Q. Zhang, *Nat. Commun.* **2017**, *8*, 181.
[30] X. Yu, J. Tang, C. Lei, C. Xue, G. Cheng, C. Xiao, H. Yang, *J. Mater. Chem. A* **2024**, *12*, 19513
[31] C. He, Y. Tang, L. A. Mitchell, D. A. Parrish, J. M. Shreeve, *J. Mater. Chem. A* **2016**, *4*, 8969.
[32] Q. Yu, Z. Wang, H. Yang, B. Wu, Q. Lin, X. Ju, C. Lu, G. Cheng, *RSC Adv.* **2015**, *5*, 27305.
[33] T. M. Klapötke, C. MiróSabate, and J. Stierstorfer, *New J. Chem.* **2009**, *33*, 136.
[34] N. Fischer, T. M. Klapötke, J. Stierstorfer, *Z. Anorg. Allg. Chem.* **2009**, *635*, 271.
[35] M. Göbel, K. Karaghiosoff, T. M. Klapötke, D. G. Piercey, J. Stierstorfer, *J. Am. Chem. Soc.* **2010**, *132*, 17216.
[36] T. M. Klapötke, C. Pflüger, *Z. Anorg. Allg. Chem.* **2017**, *643*, 619.
[37] P. Yin, D. A. Parrish, J. M. Shreeve, *J. Am. Chem. Soc.* **2015**, *137*, 4778.
[38] Q. Lang, Q. Sun, Q. Wang, Q. Lin, M. Lu, *J. Mater. Chem. A* **2020**, *8*, 11752.
[39] C. He, H. Gao, G. H. Imler, D. A. Parrish, J. M. Shreeve, *J. Mater. Chem. A* **2018**, *6*, 9391.
[40] P. Chen, H. Dou, J. Zhang, C. He, S. Pang, *ACS Appl. Mater. Interfaces* **2023**, *15*, 4144.
[41] D. E. Chavez, J. C. Bottaro, M. Petrie, D. A. Parrish, *Angew. Chem. Int. Ed.* **2015**, *54*, 12973.
[42] S. Huang, J. Tian, X. Qi, K. Wang, Q. Zhang, *Chem. Eur. J.* **2017**, *23*, 12787.
[43] P. Yi, C. Lin, X. Yi, P. He, T. Wang, J. Zhang, *ACS Appl. Mater. Interfaces* **2024**, *16*, 23426.
[44] L. Hu, P. Yin, G. H. Imler, D. A. Parrish, H. Gao, J. M. Shreeve, *Chem. Commun.* **2019**, *55*, 8979.
[45] Y. Tang, J. Zhang, L. A. Mitchell, D. A. Parrish, J. M. Shreeve, *J. Am. Chem. Soc.* **2015**, *137*, 15984.
[46] G. F. Rudakov, V. P. Sinditskii, I. A. Andreeva, A. I. Botnikova, P. R. Veselkina, S. K. Kostanyan, N. V. Yudin, V. V. Serushkin, G. V. Cherkaev, O. V. Dorofeeva, *Chem. Eng. J.* **2022**, *450*, 138073.
[47] N. Fischer, L. Gao, T. M. Klapötke, J. Stierstorfer, *Polyhedron* **2013**, *51*, 201.

[48] Z. Xu, G. Cheng, H. Yang, J. Zhang, J. M. Shreeve, *Chem. Eur. J.* **2018**, *24*, 10488.
[49] J. Ma, G. Zhang, H. Gu, J. Tang, B. Wang, H. Yang, G. Cheng, *New J. Chem.* **2019**, *43*, 8370.
[50] P. Yin, C. He, J. M. Shreeve, *Chem. Eur. J.* **2016**, *22*, 2108.
[51] Y. Joo, J. M. Shreeve, *Angew. Chem. Int. Ed.* **2009**, *48*, 564.
[52] M. Wu, S. Chen, Q. Shu, L. Li, S. Jin, *Propellants Explos. Pyrotech.* **2013**, *38*, 658.
[53] I. L. Dalinger, K. Y. Suponitsky, T. K. Shkineva, D. B. Lempertc, A. B. Sheremetev, *J. Mater. Chem. A* **2018**, *6*, 14780.
[54] Q. Ma, H. Gu, J. Huang, F. Nie, G. Fan, L. Liao, Wei Yang, *New J. Chem.* **2018**, *42*, 2376.
[55] J. Li, Y. Liu, W. Ma, T. Fei, C. He, S. Pang, *Nat. Commun.* **2022**, *13*, 5697.
[56] H. Wei, H. Gao, J. M. Shreeve, *Chem. Eur. J.* **2014**, *20*, 16943.
[57] D. Fischer, J. L. Gottfried, T. M. Klapötke, K. Karaghiosoff, J. Stierstorfer, T. G. Witkowski, *Angew. Chem. Int. Ed.* **2016**, *55*, 16132.
[58] L. Hu, P. Yin, G. Zhao, C. He, G. H. Imler, D. A. Parrish, H. Gao, J. M. Shreeve, *J. Am. Chem. Soc.* **2018**, *140*, 15001.
[59] Y. Wang, J. Ye, N. Yang, H. Ma, Y. Zhang, Z. Guo, *CrystEngComm*. **2021**, *23*, 7635.
[60] M. Zhang, H. Gao, C. Li, W. Fu, L. Tang, Z. Zhou, *J. Mater. Chem. A* **2017**, *5*, 1769
[61] J. Ma, J. Tang, H. Yang, Z. Yi, G. Wu, S. Zhu, W. Zhang, Y. Li, G. Cheng, *ACS Appl. Mater. Interfaces* **2019**, *11*, 26053.
[62] A. K. Chinnam, J. Singh, R. J. Staples, J. M. Shreeve, *Chem. Eng. J.* **2022**, *433*, 133520.
[63] W. Fu, B. Zhao, M. Zhang, C. Li, H. Gao, J. Zhang, Z. Zhou, *J. Mater. Chem. A* **2017**, *5*, 5044.
[64] Z. Xu, G. Cheng, H. Yang, X. Ju, P. Yin, J. Zhang, J. M. Shreeve, *Angew. Chem. Int. Ed.* **2017**, *56*, 5877.
[65] L. Qian, H. Yang, H. Xiong, H. Gu, J. Tang, Y. Xue, G. Cheng, *Energ. Mater. Front.* **2020**, *1*, 74.
[66] Y. Tang, C. He, P. Yin, G. H. Imler, D. A. Parrish, J. M. Shreeve, *Eur. J. Org. Chem.* **2018**, *2018*, 2273.
[67] T. Yan, H. Yang, G. Cheng, *ACS Appl. Energy Mater.* **2020**, *3*, 6492.
[68] G. Herve, C. Roussel, H. Graindorge, *Angew. Chem. Int. Ed.* **2010**, *49*, 3177.
[69] T. S. Hermann, T. M. Klapötke, B. Krumm, J. Stierstorfer, *New J. Chem.* **2017**, *41*, 3068.
[70] A. A. Voronin, I. V. Fedyanin, A. M. Churakov, A. N. Pivkina, N. V. Muravyev, Y. A. Strelenko, M. S. Klenov, D. B. Lempert, V. A. Tartakovsky, *ACS Appl. Energy Mater.* **2020**, *3*, 9401.
[71] P. Yin, J. M. Shreeve, *Angew. Chem. Int. Ed.* **2015**, *54*, 14513.
[72] Q. Wang, Y. Shao, M. Lu, *Cryst. Growth Des.* **2018**, *18*, 6150.
[73] L. Hu, C. He, G. Zhao, G. H. Imler, D. A. Parrish, J. M. Shreeve, *ACS Appl. Energy Mater.* **2020**, *3*, 5510.
[74] L. L. Fershtat, I. V. Ovchinnikov, M. A. Epishina, A. A. Romanova, D. B. Lempert, N. V. Muravyev, N. N. Makhova, *ChemPlusChem* **2017**, *82*, 1315.
[75] V. Thottempudi, H. Gao, J. M. Shreeve, *J. Am. Chem. Soc.* **2011**, *133*, 6464.
[76] P. Yang, H. Yang, Y. Zhao, J. Tang, G. Cheng, *Dalton Trans.* **2021**, *50*, 16499.
[77] P. Yin, J. Zhang, G. H. Imler, D. A. Parrish, J. M. Shreeve, *Angew. Chem. Int. Ed.* **2017**, *56*, 8834.
[78] X. X. Zhao, S. H. Li, Y. Wang, Y. C. Li, F. Q. Zhao, S. P. Pang, *J. Mater. Chem. A* **2016**, *4*, 5495.
[79] J. Ma, A. K. Chinnam, G. Cheng, H. Yang, J. Zhang, J. M. Shreeve, *Angew. Chem. Int. Ed.* **2021**, *60*, 5497.
[80] G. Zhang, C. Xiao, Z. Dong, M. Lv, Y. Liu, X. Hao, Y. Zou, H. Zhang, Z. Ye, *Cryst. Growth Des.* **2023**, *23*, 6756.

[81] Y.-H. Joo, J. M. Shreeve, *Angew. Chem. Int. Ed.* **2010**, *49*, 7320.
[82] N. V. Muravyev, K. Y. Suponitsky, I. V. Fedyanin, I. V. Fomenkov, A. N. Pivkina, I. L. Dalinger, *Chem. Eng. J.* **2022**, *449*, 137816.
[83] Z. Jiang, N. Ding, Q. Sun, C. Zhao, B. Tian, S. Li, S. Pang, *Chem. Eng. J.* **2023**, *473*, 145331.
[84] Y. Tang, H. Gao, L. A. Mitchell, D. A. Parrish, J. M. Shreeve, *Angew. Chem. Int. Ed.* **2016**, *55*, 3200.
[85] X. Huang, L. Chen, H. Huang, J. Yang, *Energ. Mater. Front.* **2023**, *4*, 221.
[86] G. Wang, T. Lu, G. Fan, C. Li, H. Yin, F.-X. Chen, *Chem. Asian J.* **2018**, *13*, 3718.
[87] K. Mohammad, V. Thaltiri, N. Kommu, A. A. Vargeese, *Chem. Commun.* **2020**, *56*, 12945.
[88] S. Dharavath, J. Zhang, G. H. Imler, D. A. Parrish, J. M. Shreeve, *J. Mater. Chem. A* **2017**, *5*, 4785.
[89] Y Wang, Y. Liu, S. Song, Z. Yang, X. Qi, K. Wang, Y. Liu, Q. Zhang, Y. Tian, *Nat. Commun.* **2018**, *9*, 2444.
[90] C. Li, M. Zhang, Q. Chen, Y. Li, H. Gao, W. Fu, Z. Zhou, *Dalton Trans.* **2016**, *45*, 17956.
[91] N. Ding, Q. Sun, X. Xu, W. Zhang, C. Zhao, S. Li, S. Pang, *J. Org. Chem.* **2024**, *89*, 10467.
[92] W. Li, K. Wang, X. Qi, Y. Jin, Q. Zhang, *Cryst. Growth Des.* **2018**, *18*, 1896.
[93] J. Tang, P. Yang, H. Yang, H. Xiong, W. Hu, G. Cheng, *Chem. Eng. J.* **2020**, *386*. 124027.
[94] H. Xiong, H. Yang, G. Cheng, *New J. Chem.* **2019**, *43*, 13827.
[95] Q. Yu, G. H. Imler, D. A. Parrish, J. M. Shreeve, *Org. Lett.* **2019**, *21*, 4684.
[96] T. M. Klapötke, P. Mayer, J. Stierstorfera, J. J. Weigand, *J. Mater. Chem.* **2008**, *18*, 5248.
[97] Y. Feng, M. Deng, S. Song, S. Chen, Q. Zhang, J. M. Shreeve, *Engineering* **2020**, *6*, 1006.
[98] Q. J. Axthammer, B. Krumm, T. M. Klapötke, R. Scharf, *Chem. Eur. J.* **2015**, *21*, 16229.
[99] W. Zhang, Y. Yang, S. Shi, S. Pang, Y. Li, C. Sun, *Phys. Chem. Chem. Phys.* **2023**, *25*, 20168.
[100] M. Deng, Y. Feng, W. Zhang, X. Qi, Q. Zhang, *Nat. Commun.* **2019**, *10*, 1339.
[101] C. Li, T. Zhu, C. Lei, G. Cheng, C. Xiao, H. Yang, *J. Mater. Chem. A* **2023**, *11*, 12043.
[102] S. Feng, B. Zhang, C. Luo, Y. Liu, S. Zhu, R. Gou, S. Zhang, P. Yin, S. Pang, *Org. Lett.* **2023**, *25*, 1290.
[103] S. Zhang, G. Cheng, H. Yang, *Dalton Trans.* **2020**, *49*, 5590.
[104] B. Wang, X. Qi, W. Zhang, K. Wang, W. Li, Q. Zhang, *J. Mater. Chem. A* **2017**, *5*, 20867.
[105] Z. Fu, R. Su, Y. Wang, Y.-F. Wang, W. Zeng, N. Xiao, Y. Wu, Z. Zhou, J. Chen, F.-X. Chen, *Chem. Eur. J.* **2012**, *18*, 1886.
[106] T. M. Klapötke, A. Penger, C. Pflüger, J. Stierstorfer, M. Suceska, *Eur. J. Inorg. Chem.*, **2013**, *2013*, 4667.
[107] T. M. Klapötke, D. G. Piercey, J. Stierstorfer, *Dalton Trans.* **2012**, *41*, 9451.
[108] J. Ma, H. Yang, J. Tang, G. Zhang, Z. Yi, S. Zhu, G. Cheng, *Dalton Trans.* **2020**, *49*, 4675.
[109] T. M. Klapötke, B. Krumm, R. Scharf, *Z. Anorg. Allg. Chem.* **2016**, *642,* 887.
[110] Q. Ma, G. Zhang, J. Li, Z. Zhang, H. Lu, L. Liao, G. Fan, F. Nie, *Chem. Eng. J.* **2020**, *379*, 122331.
[111] Q. Yu, J. Singh, R. J. Staples, J. M. Shreeve, *Chem. Eng. J.* **2022**, *431*, 133235.
[112] D. R. Wozniak, B. Salfer, M. Zeller, E. F. C. Byrd, D. G. Piercey, *Org. Lett.* **2020**, *22*, 9114.
[113] Z. Xu, G. Cheng, S. Zhu, Q. Lin, H. Yang, *J. Mater. Chem. A* **2018**, *6*, 2239.
[114] S. Chen, L. Li, S. Song, Q. Zhang, *Cryst. Growth Des.* **2023**, *23*, 4970.
[115] J. Ma, A. K. Chinnam, G. Cheng, H. Yang, J. Zhang, J. M. Shreeve, *Angew. Chem. Int. Ed.* **2021**, *60*, 5497.
[116] P. Yin, J. Zhang, C. He, D. A. Parrish, J. M. Shreeve, *J. Mater. Chem. A* **2014**, *2*, 3200.
[117] T. Lu, C. Wang, G. Wang, S. Wang, J. Song, H. Yin, G. Fan, F.-X. Chen, *New J. Chem.* **2019**, *43*, 13330.

[118] Q. Sun, C. Shen, X. Li, Q. Lin, M. Lu, *Cryst. Growth Des.* **2017**, *17*, 6105.
[119] Q. Yu, A. K. Chinnam, P. Yin, G. H. Imler, Damon A. Parrishc, J. M. Shreeve, J. Mater. Chem. A 2020, 8, 5859.
[120] P. W. Leonard, C. J. Pollard, D. E. Chavez, B. M. Rice, D. A. Parrish, *Synlett.* **2011**, *14*, 2097.
[121] Y. Du, J. Zhang, P. Peng, H. Su, S. Li, S. Pang, *New J. Chem.* **2017**, *41*, 9244.
[122] T. Liu, X. Qi, K. Wang, J. Zhang, W. Zhang, Q. Zhang, *New J. Chem.* **2017**, *41*, 9070.
[123] V. Thaltiri, J. Singh, R. J. Staples, J. M. Shreeve, *J. Mater. Chem. A* **2024**, *12*, 9546.
[124] S. Chen, Y. Liu, Y. Feng, X. Yang, Q. Zhang, *Chem. Commun.* **2020**, *56*, 1493.
[125] A. Shlomovich, T. Pechersky, A. Cohen, Q. L. Yan, M. Kosa, N. Petrutik, N. Tal, A. Aizikovich, M. Gozin, *Dalton Trans.* **2017**, *46*, 5994.
[126] F. Yang, P. Zhang, X. Zhou, Q. Lin, P. Wang, M. Lu, *Cryst. Growth Des.* **2020**, *20*, 3737.
[127] Q. Wang, Y. Shao, M. Lu, *Chem. Commun.* **2019**, *55*, 6062.
[128] A. B. Sheremetev, V. L. Korolev, A. A. Potemkin, Na. S. Aleksandrova, N. V. Palysaeva, T. H. Hoang, V. P. Sinditskii, K. Y. Suponitsky, *Asian J. Org. Chem.* **2016**, *5*, 1388.
[129] J. Li, X. Zhang, Y. Wang, D. Su, S. Pang, C. He, *New J. Chem.* **2024**, *48*, 1067.
[130] X. Zheng, T. Yan, G. Cheng, H. Yang, *Chem. Eng. J.* **2023**, *460*, 141654.
[131] Q. Yu, Z. Wang, B. Wu, H. Yang, X. Ju, C.Lu, G. Cheng, *J. Mater. Chem. A* **2015**, *3*, 8156.
[132] M. C. Schulze, B. L. Scott, D. E. Chavez, *J. Mater. Chem. A* **2015**, *3*, 17963.
[133] S. La, R. J. Staples, J. M. Shreeve, *Dalton Trans.* **2023**, *52*, 12341.
[134] S. Chen, W. Zhang, Y. Wang, Q. Zhang, *Chem. Eng. J.* **2021**, *421*, 129635.
[135] N. Ding, Q. Sun, X. Xu, Y. Li, C. Zhao, S. Li, S. Pang, *Chem. Commun.* **2023**, *59*, 1939.

9. Copies of NMR, HRMS, IR and DSC spectra of new compounds

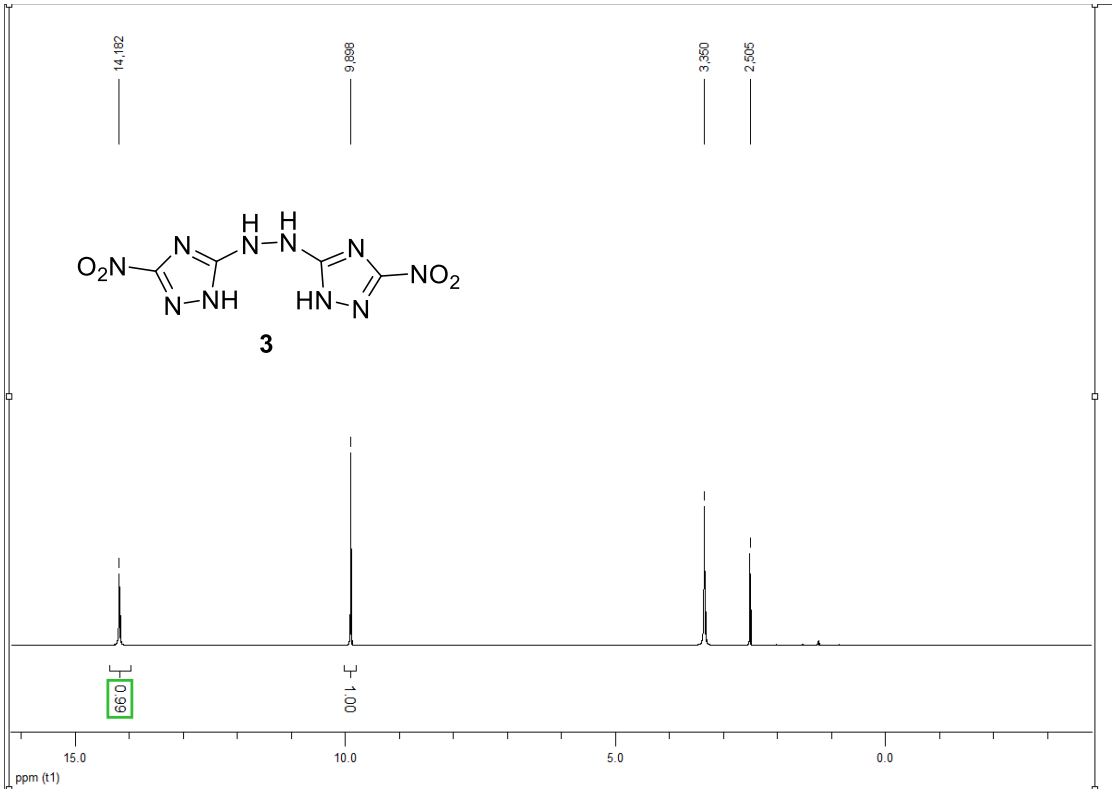

Figure S10 ^{1}H NMR spectrum of **3**.

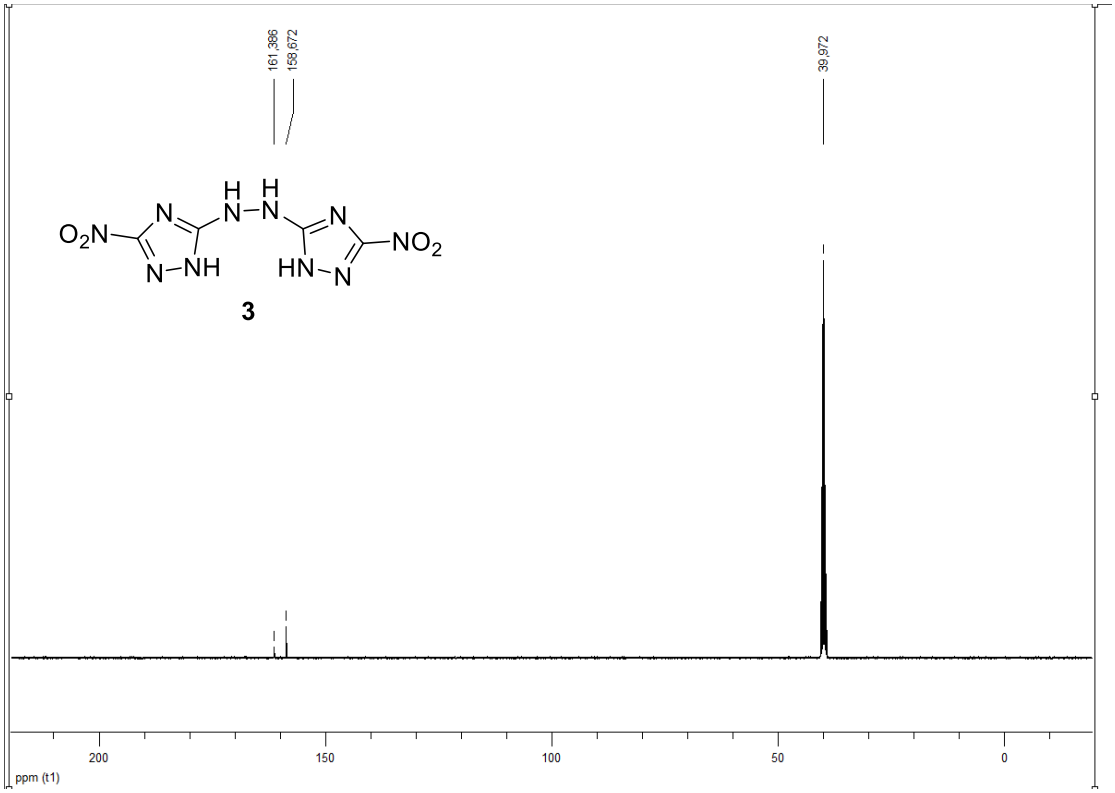

Figure S11 ^{13}C NMR spectrum of **3**.

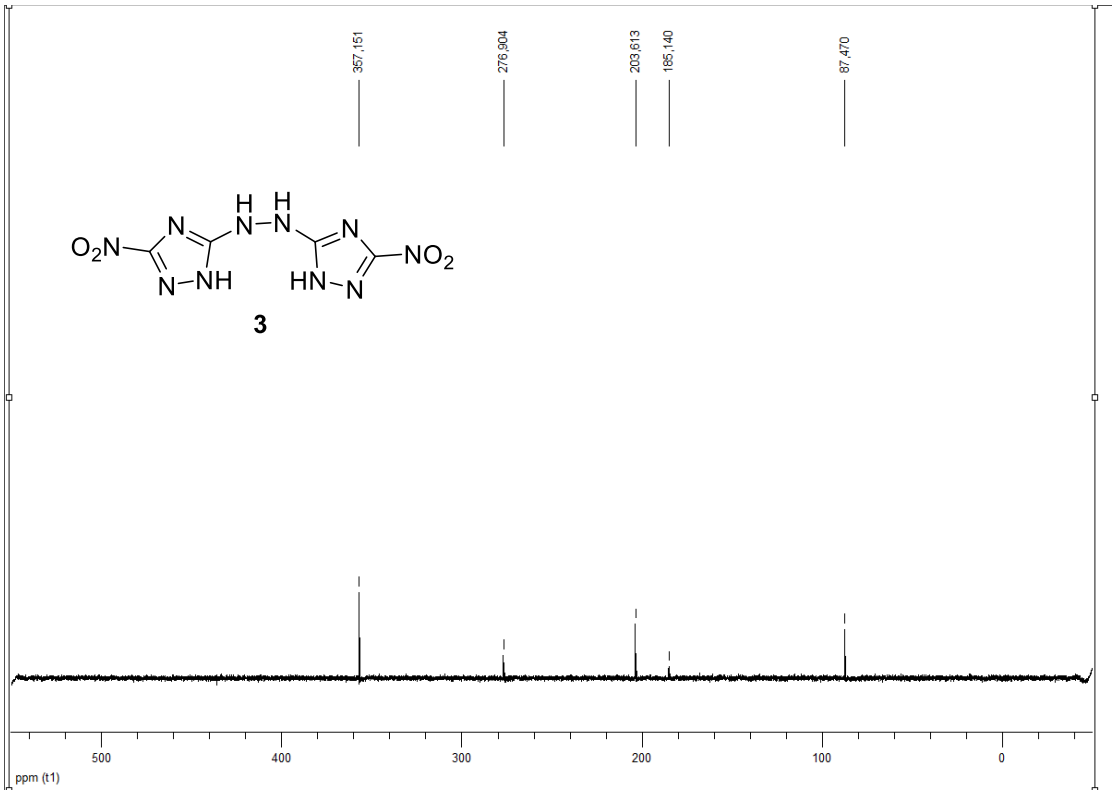

Figure S12 ^{15}N NMR spectrum of **3**.

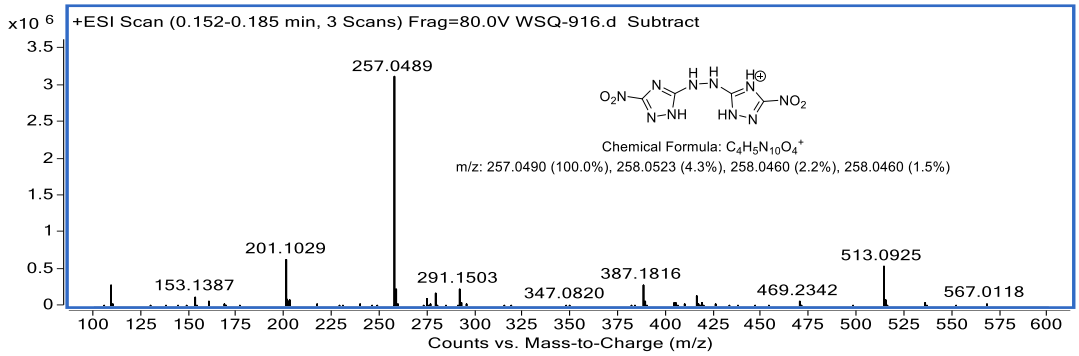

Figure S13 ESI-HRMS spectrum of **3**.

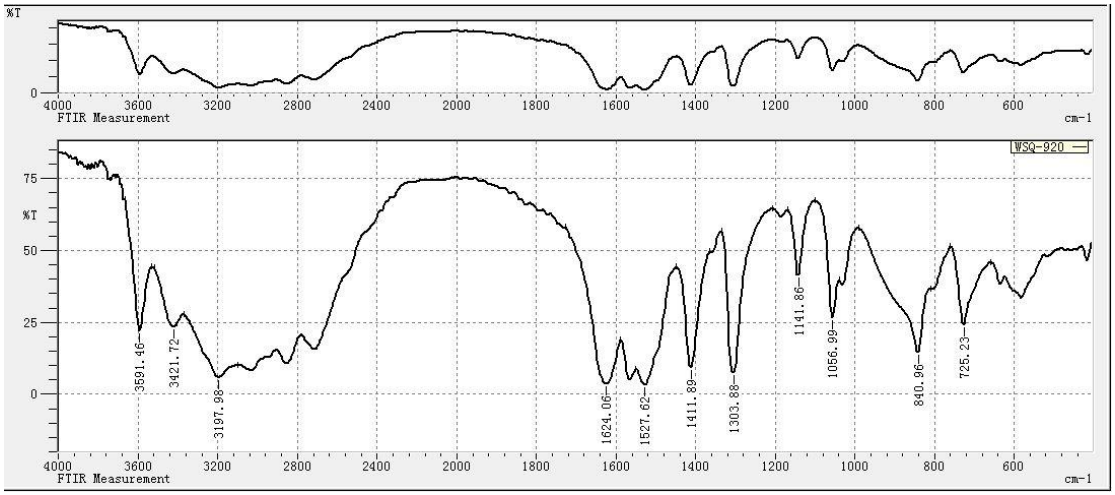

Figure S14 IR spectrum of **3**.

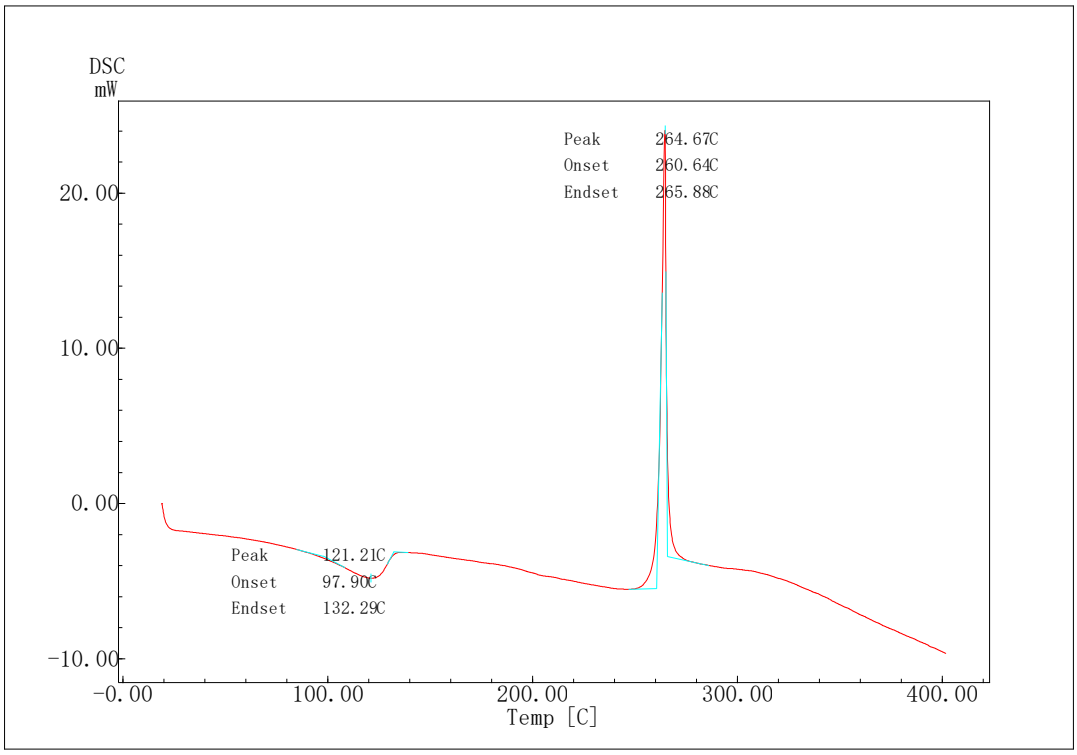

Figure S15 DSC curve of **3** (10 ºC min^{-1}).

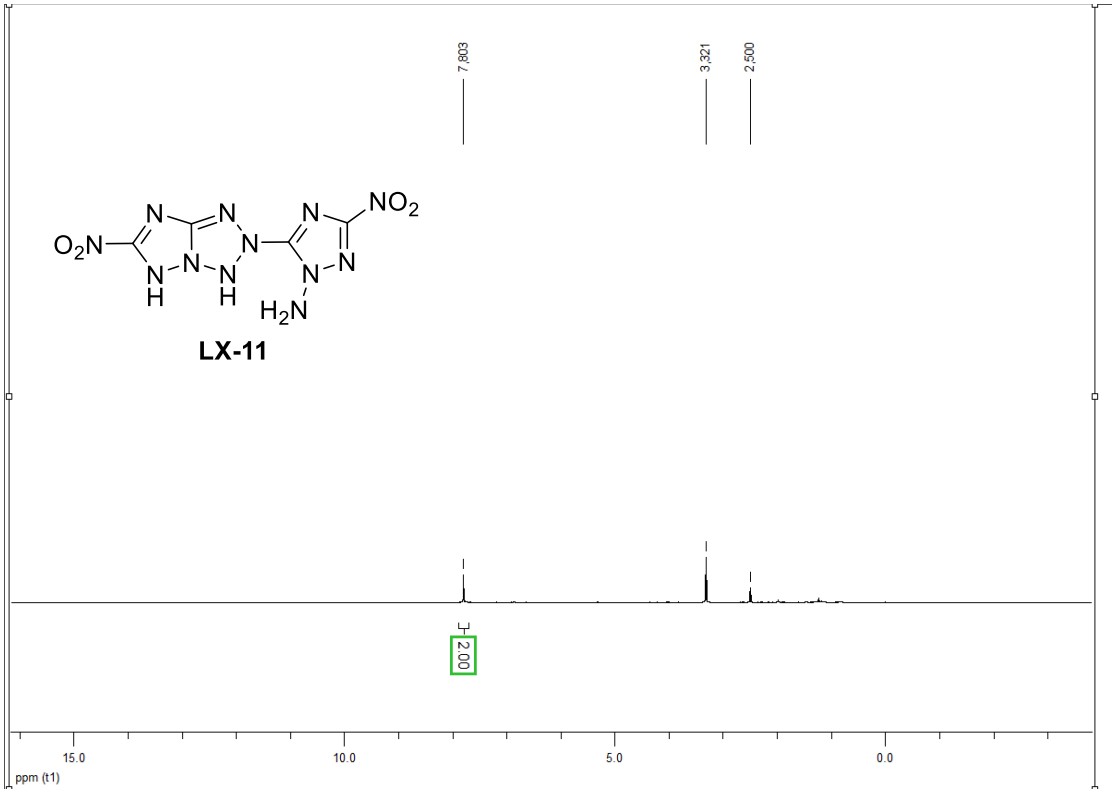

Figure S16 ^{1}H NMR spectrum of **LX-11**.

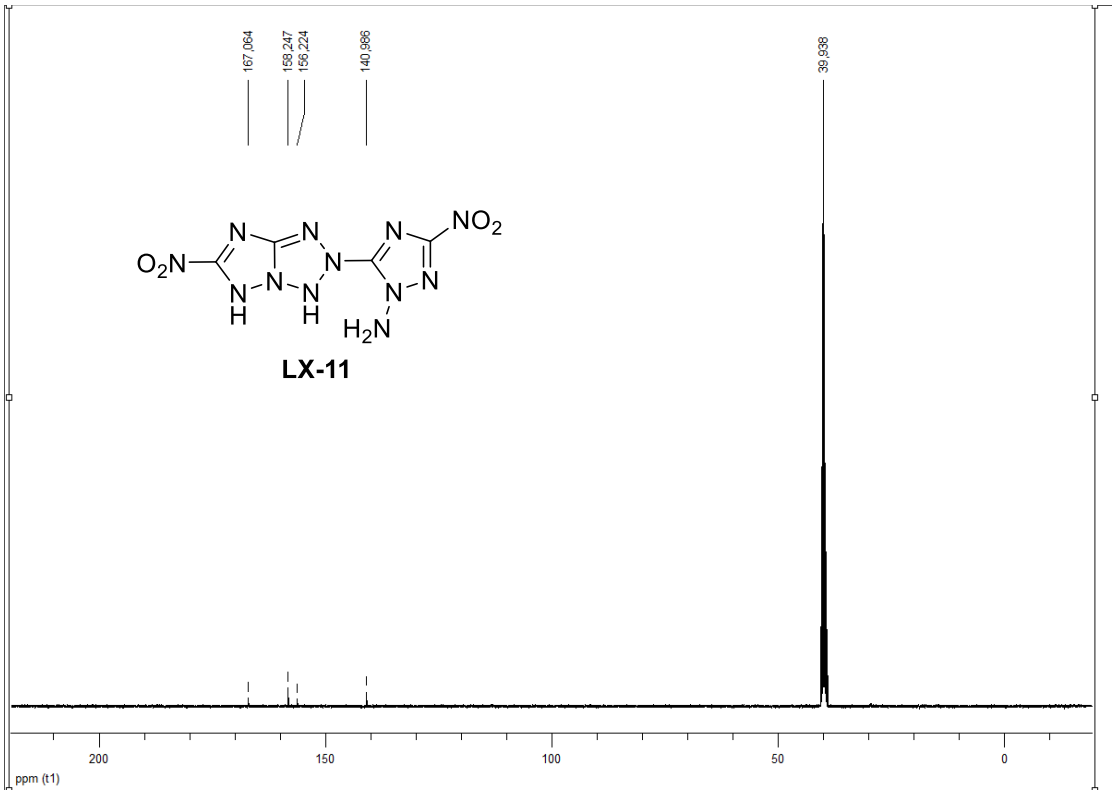

Figure S17 ^{13}C NMR spectrum of **LX-11**.

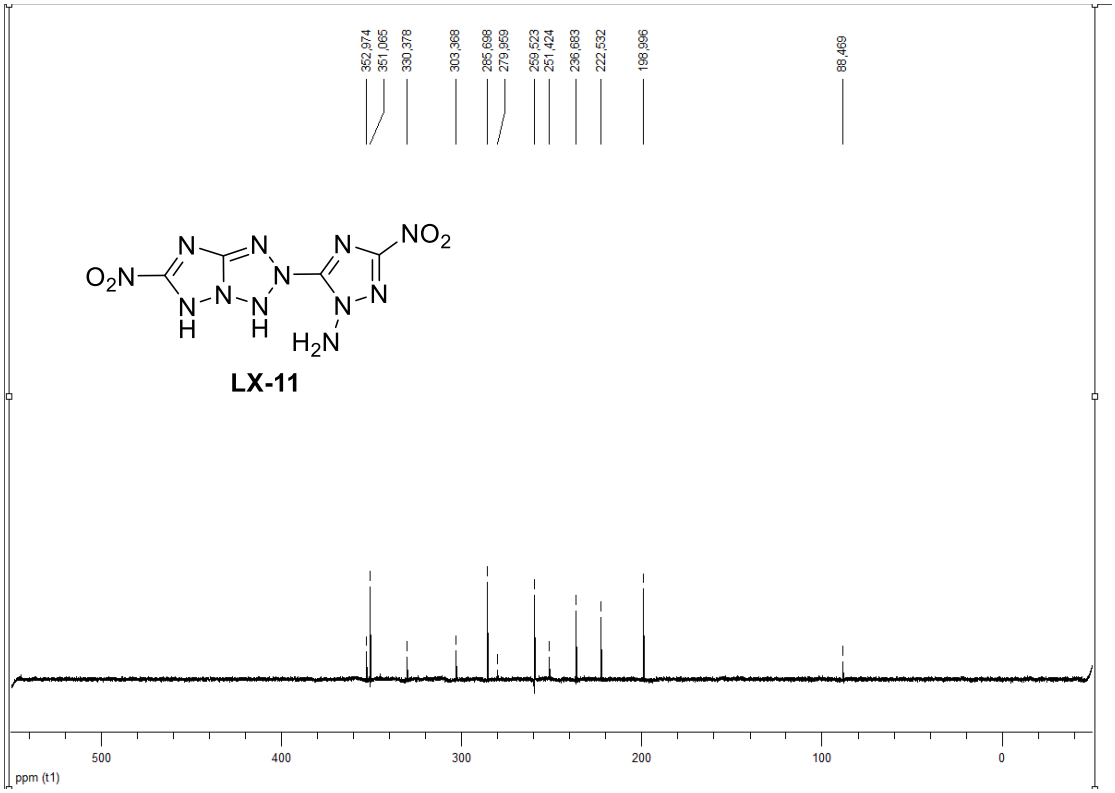

Figure S18 ^{15}N NMR spectrum of **LX-11**.

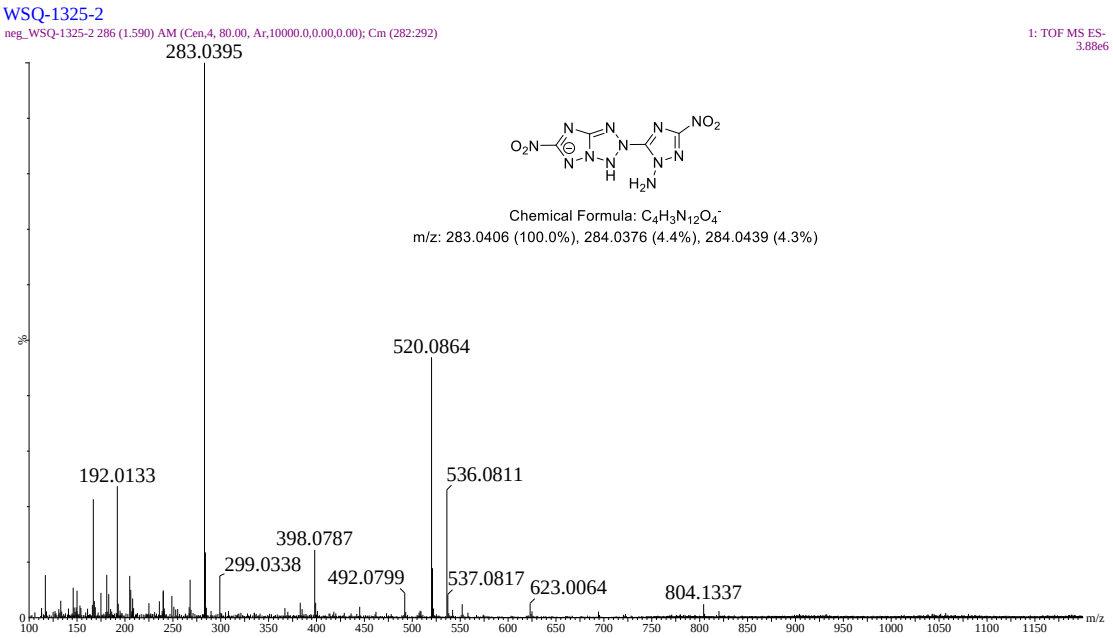

Figure S19 ESI-HRMS spectrum of **LX-11**.

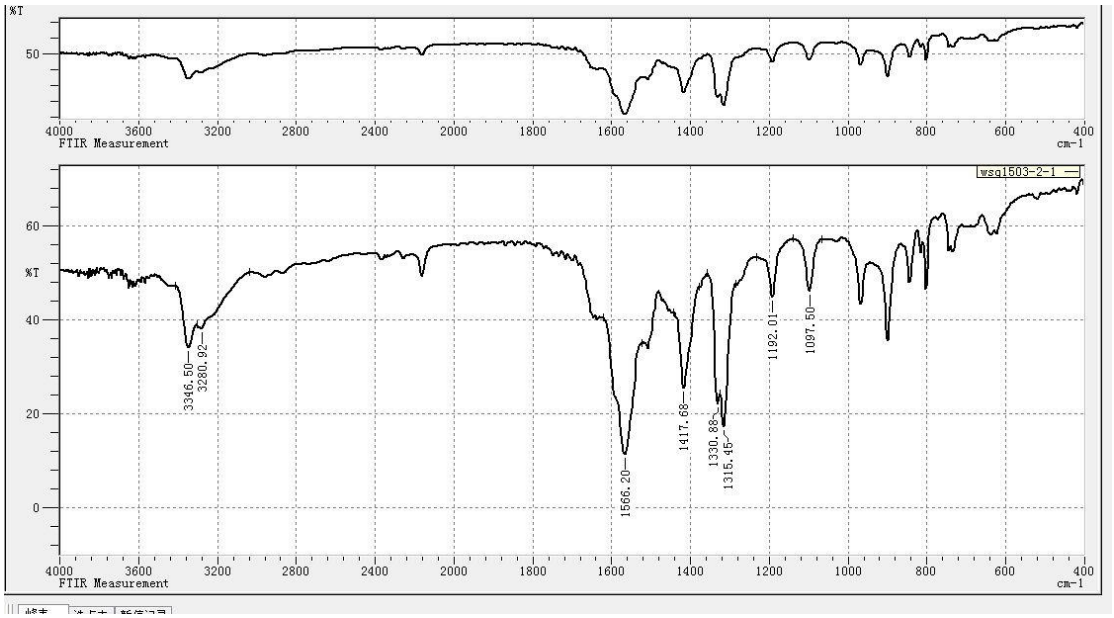

Figure S20 IR spectrum of **LX-11**.

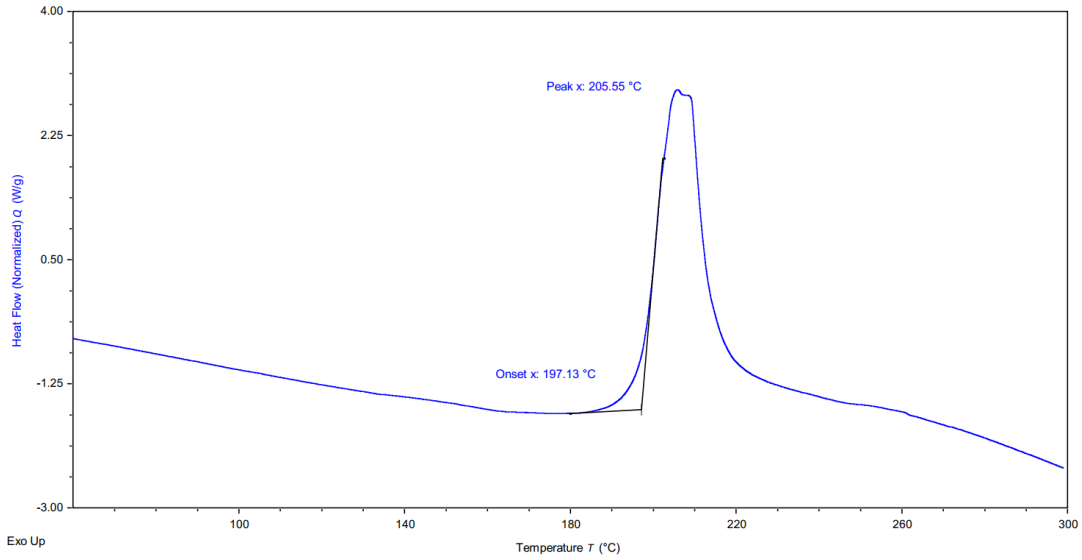

Figure S21 DSC curve of **LX-11** (2.5 ºC min^{-1}).

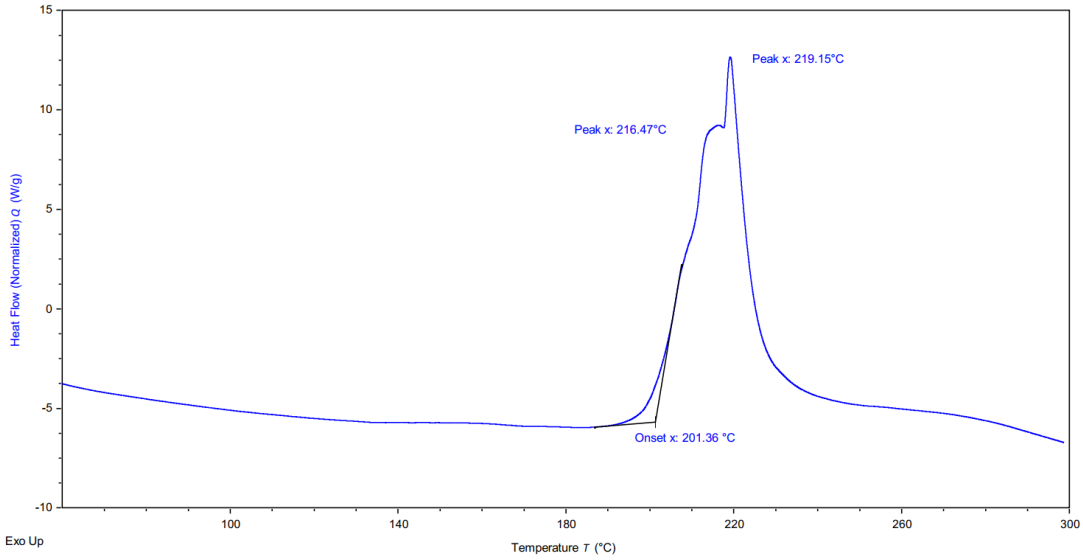

Figure S22 DSC curve of **LX-11** (5 ºC min^{-1}).

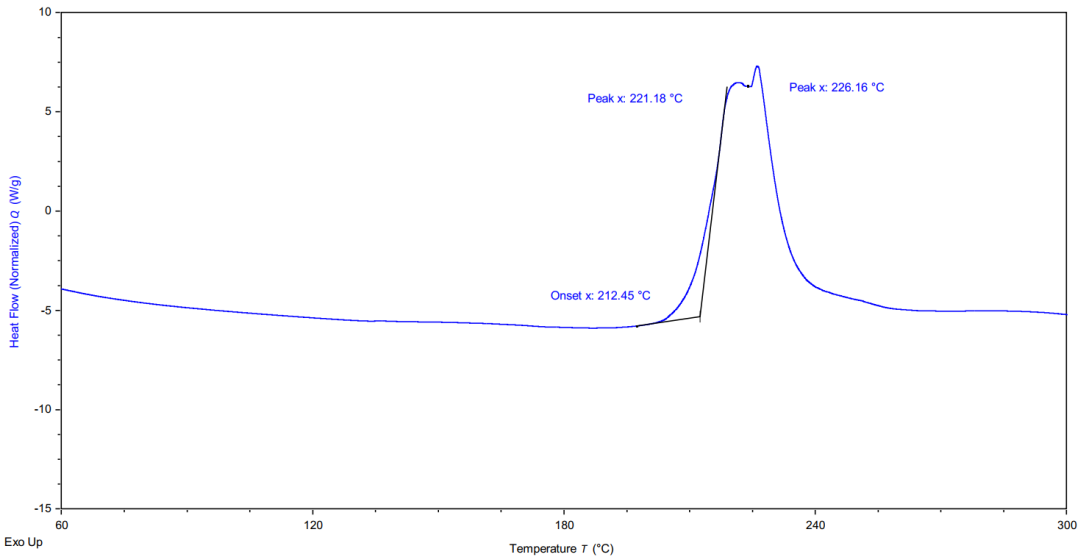

Figure S23 DSC curve of **LX-11** (10 ºC min^{-1}).

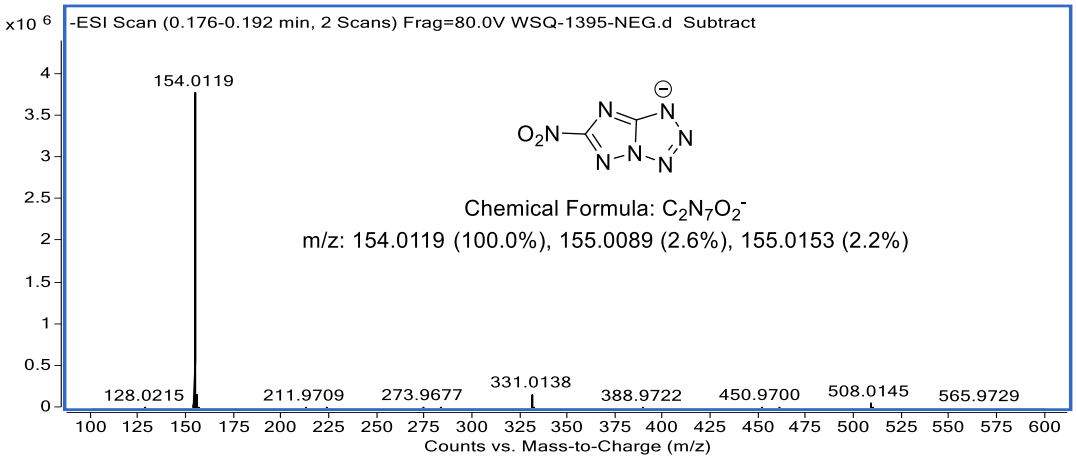

Figure S24 ESI-HRMS spectrum of **5**.

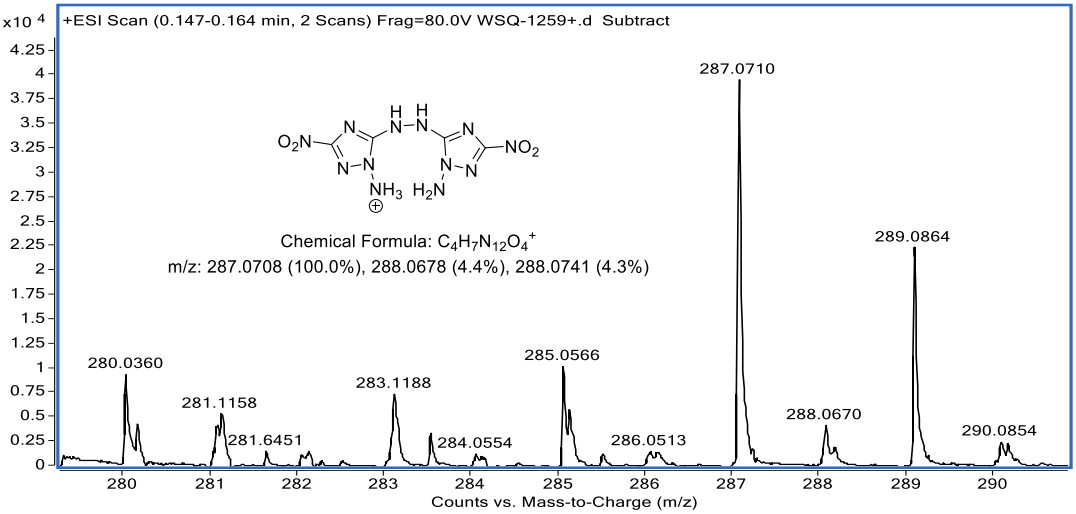

Figure S25 ESI-HRMS spectrum of **I**.

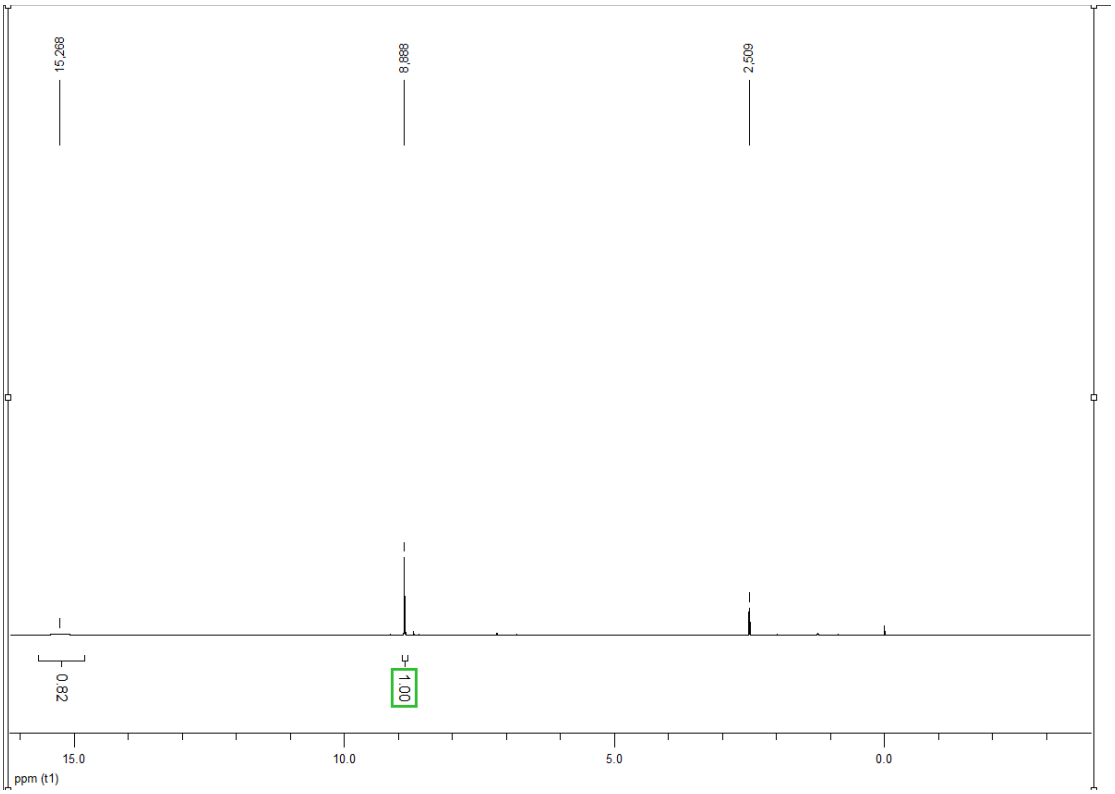

Figure S26 ^{1}H NMR spectrum of **6**.

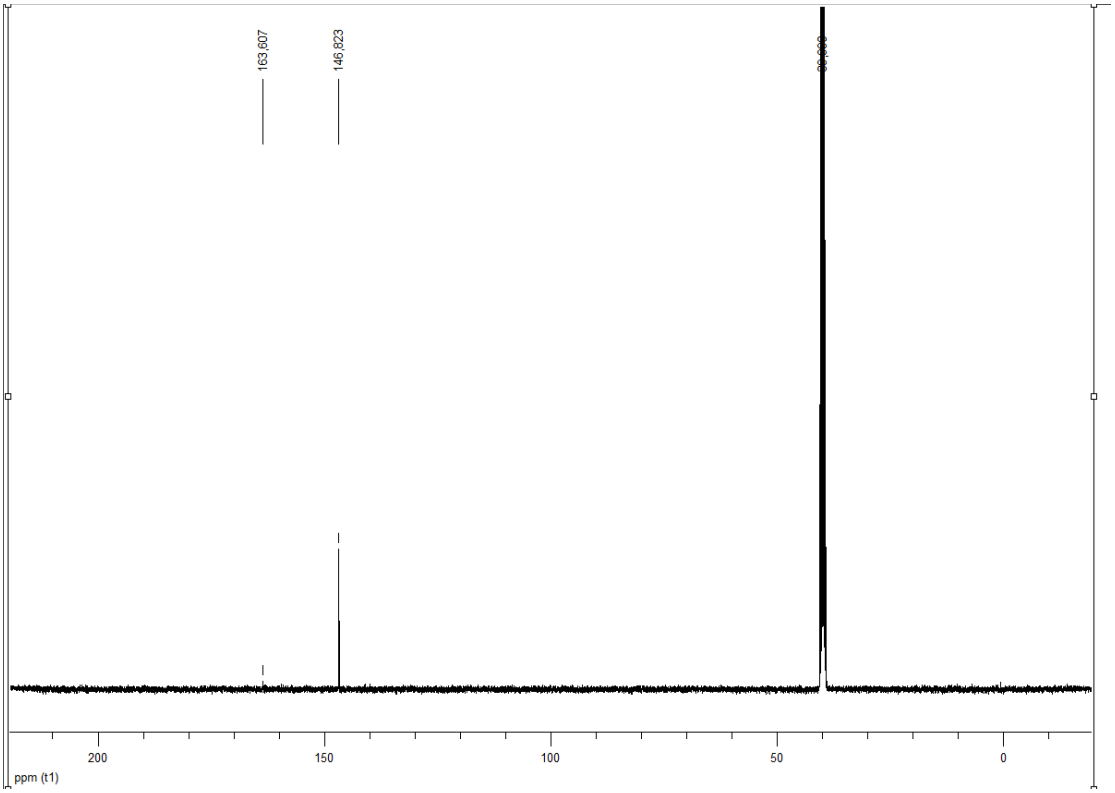

Figure S27 ^{13}C NMR spectrum of **6**.

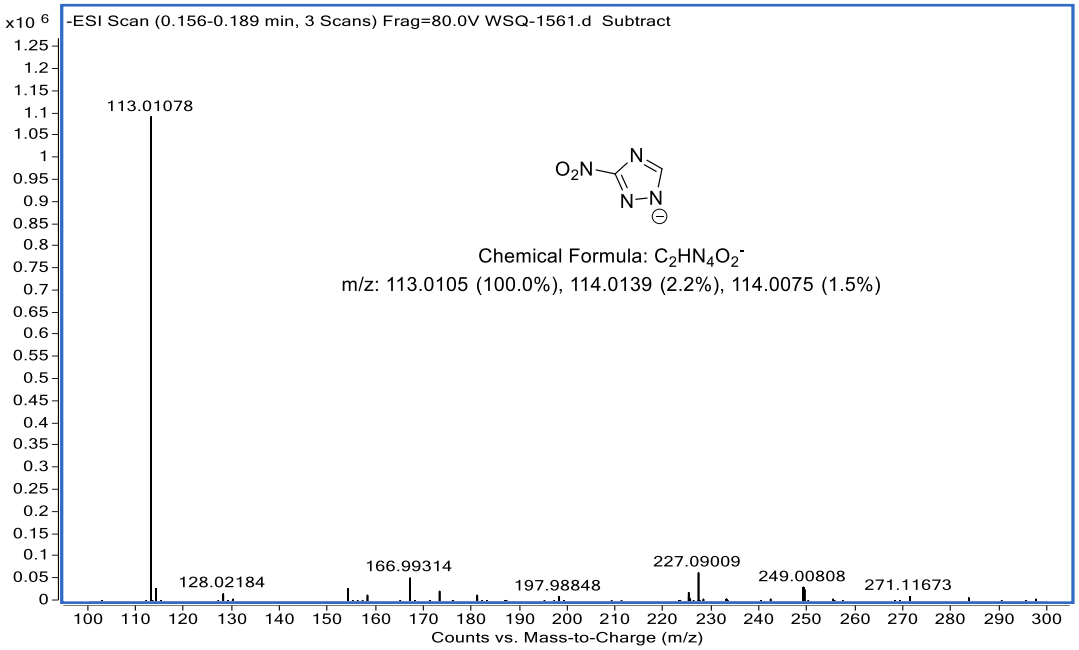

Figure S28 ESI-HRMS spectrum of **6**.

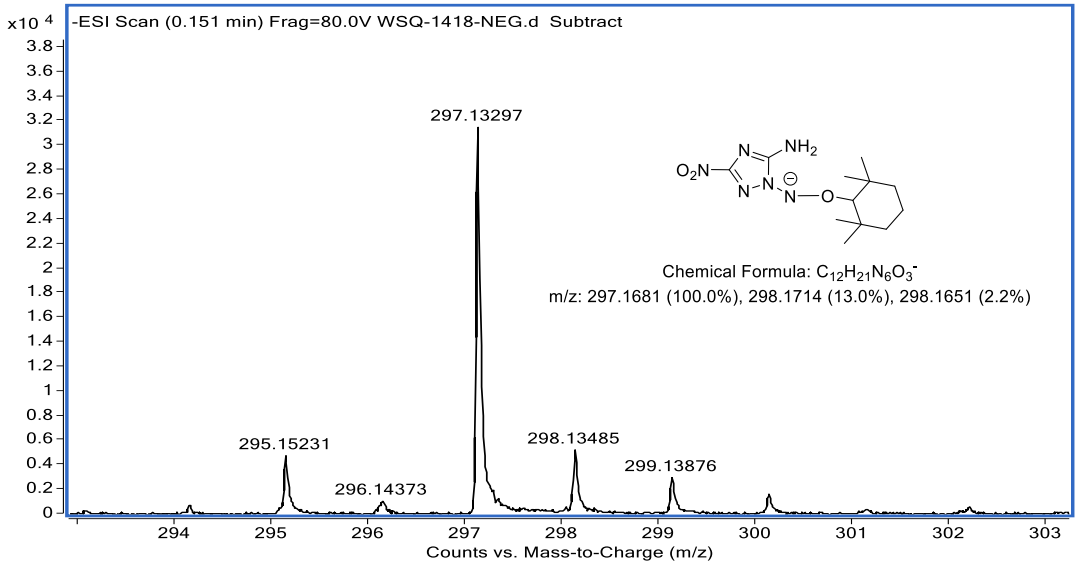

Figure S29 ESI-HRMS spectrum of TEMPO-adduct.